

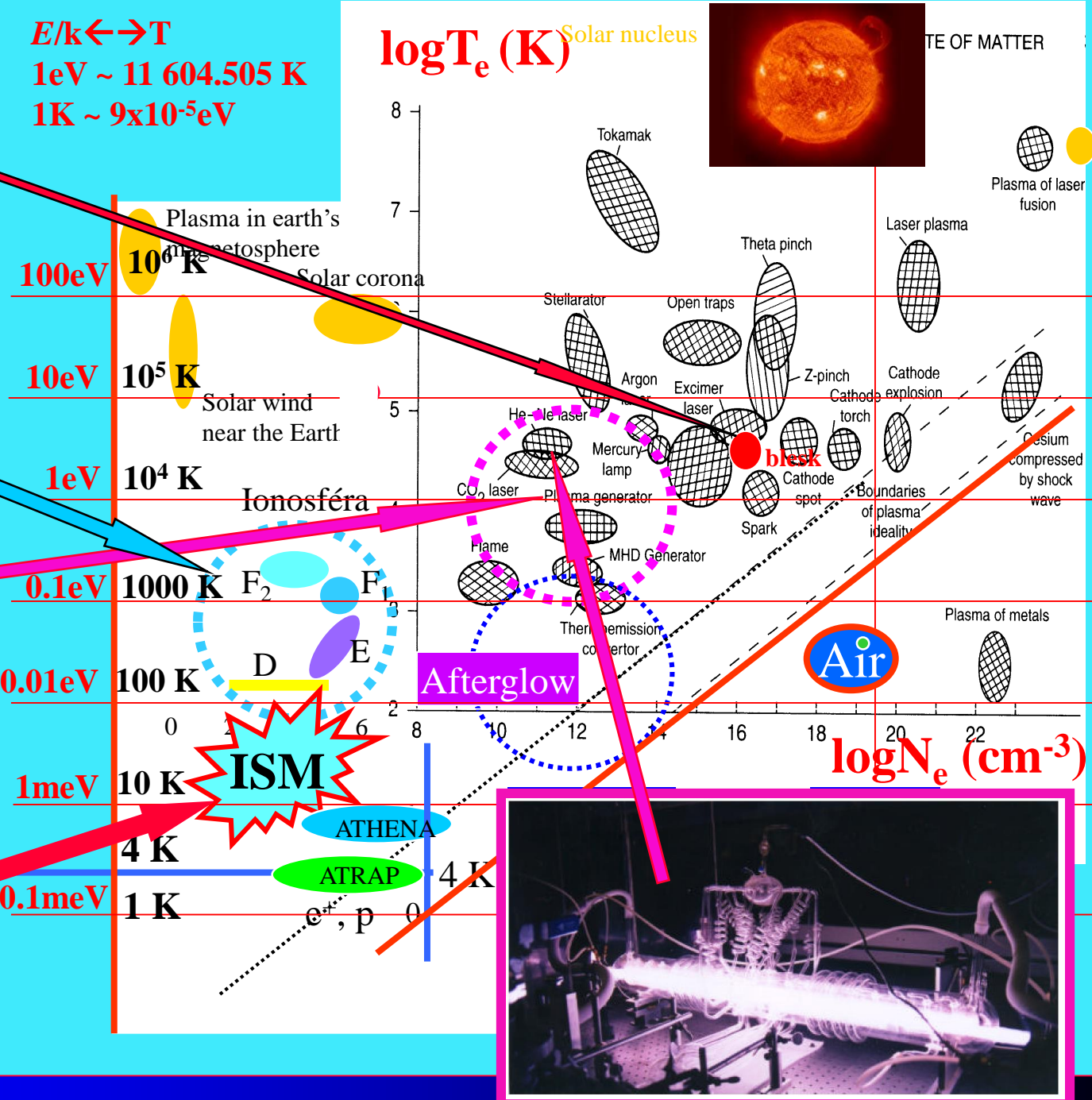
motto

If you understand hydrogen, you understand all that can be understood. V. Weisskopf
(Taken from G. Herzberg).

Temperatures and energies

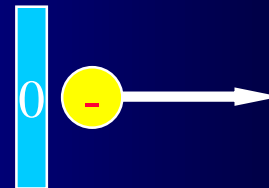


$E/k \leftrightarrow T$
 $1\text{eV} \sim 11\,604.505 \text{ K}$
 $1\text{K} \sim 9 \times 10^{-5} \text{ eV}$



Electronvolt

$$E \leftrightarrow kT$$
$$1\text{eV} \sim 11\,604.505 \text{ K}$$
$$1\text{K} \sim 9 \times 10^{-5} \text{ eV}$$

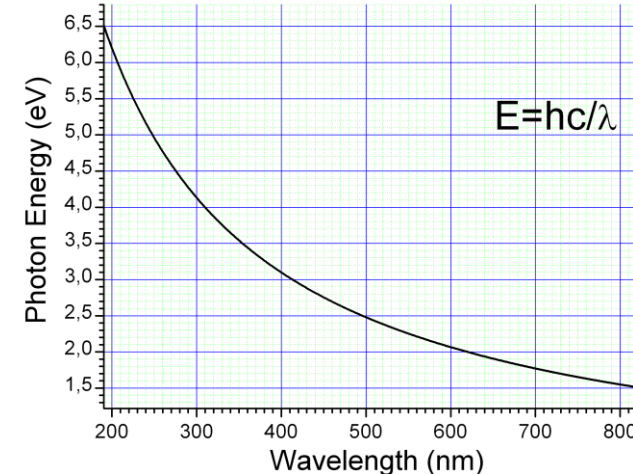
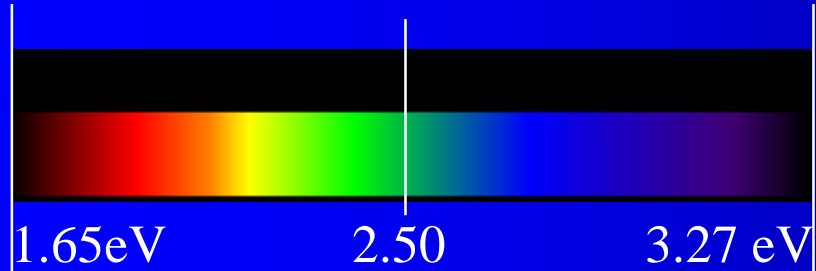


By definition, it is equal to the amount of kinetic energy gained by a single unbound electron when it accelerates through an electric potential difference of one volt

Conversion factors:

$1 \text{ eV} = 1.6021765(40) \times 10^{-19} \text{ J}$ (the conversion factor is numerically equal to the [elementary charge](#) expressed in [coulombs](#)).
 1 eV (per atom) is 96.485 kJ/mol .

1.6 to 3.4 eV: the [photon energy](#) of visible light.

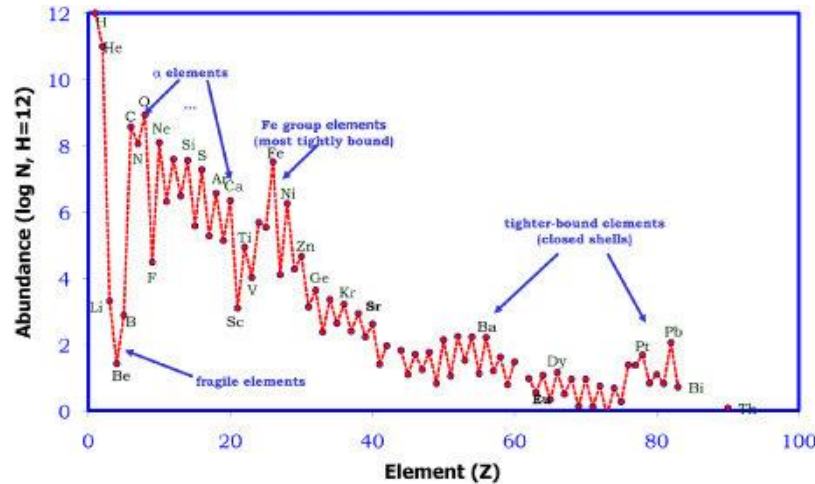


13.6 eV: The energy required to [ionize atomic hydrogen](#).

[Molecular bond energies](#) are on the [order](#) of one eV per molecule

1 TeV: A trillion electronvolts, or $1.602 \times 10^{-7} \text{ J}$, about the kinetic energy of a flying [mosquito](#)

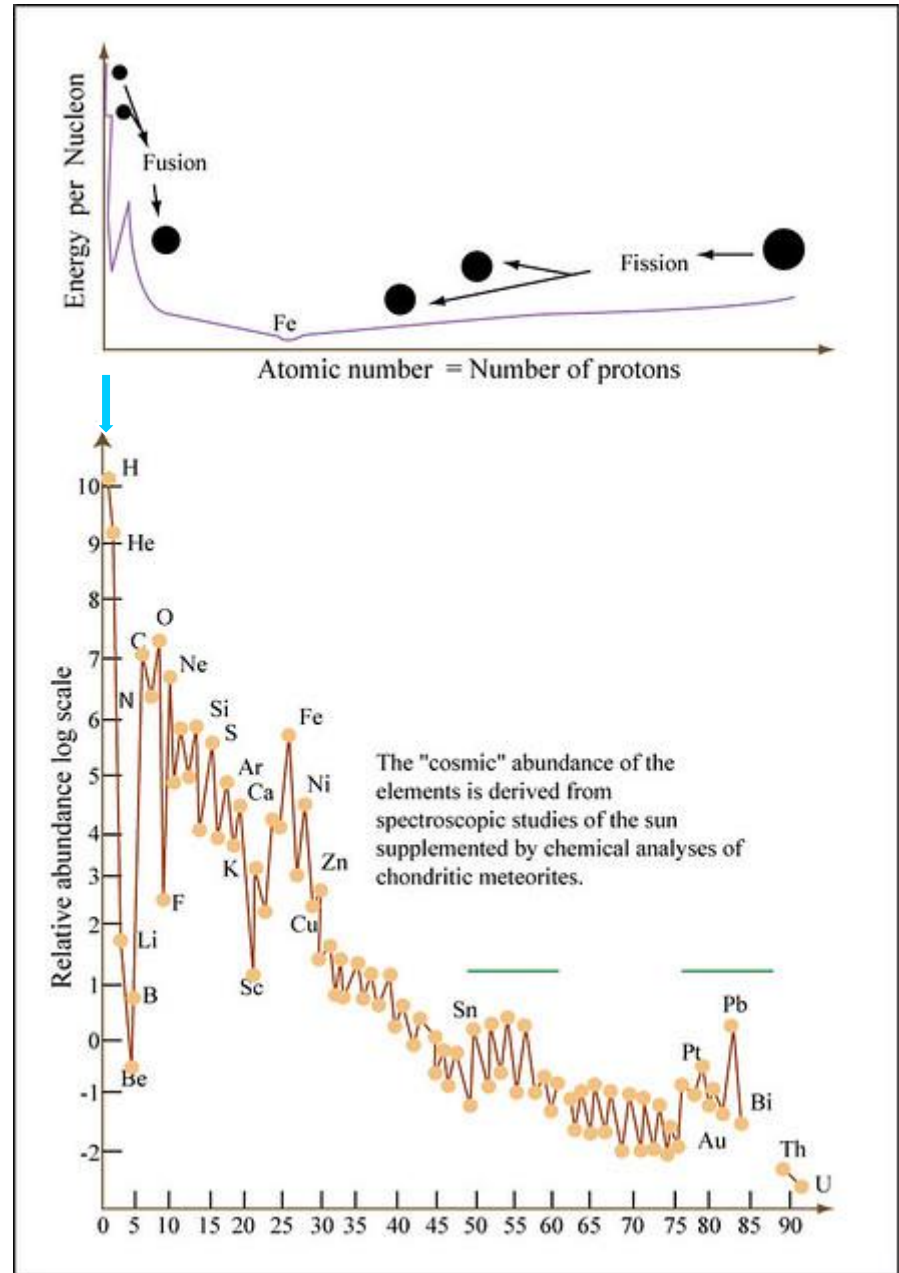
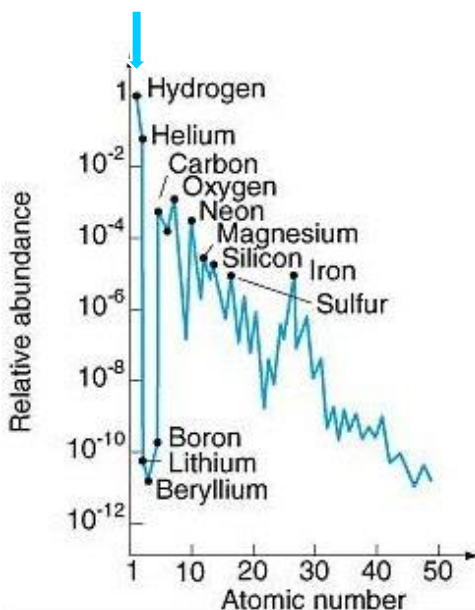
14 TeV: the design proton collision energy at the [Large Hadron Collider](#) (which has operated at half of the energy since March 30, 2010).



92.1% of nucleons in the universe are protons

7.8% are helium nuclei !

0.1%.....C,N,O,S,Si....



The cosmic elemental abundances extend over 12 orders of magnitude.

Interstellar medium

92.1% of nucleons in the universe are protons

7.8% are helium nuclei !

0.1%.....C,N,O,S,Si....

Cosmic abundance

H

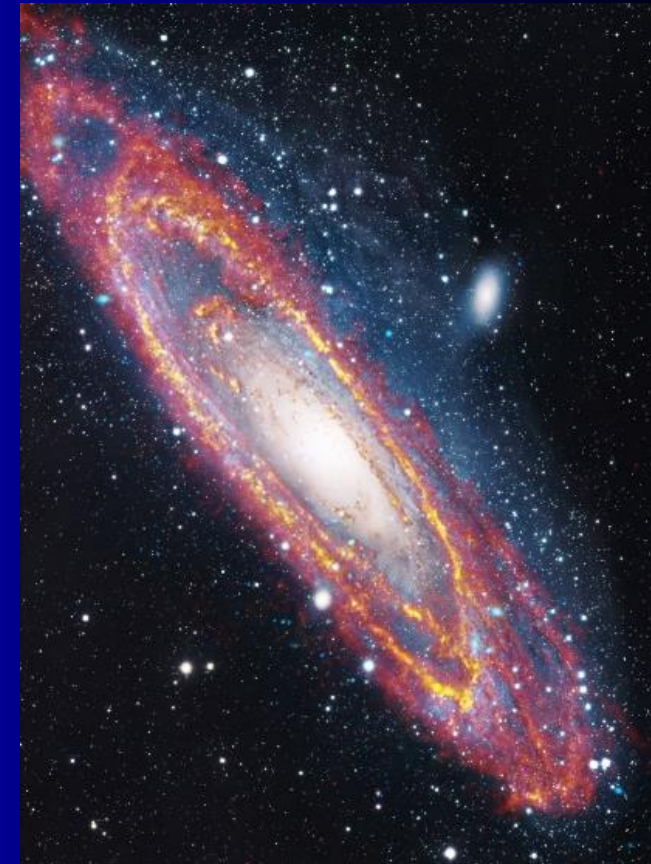
He

· · · ·
C N O Ne

Mg

· · · ·
Si S Ar

Fe



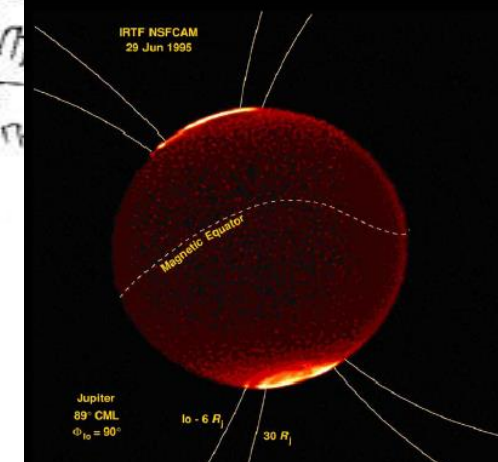
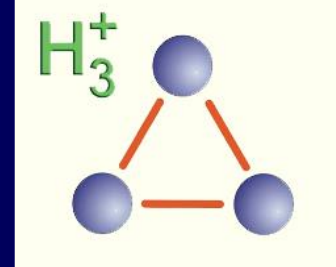
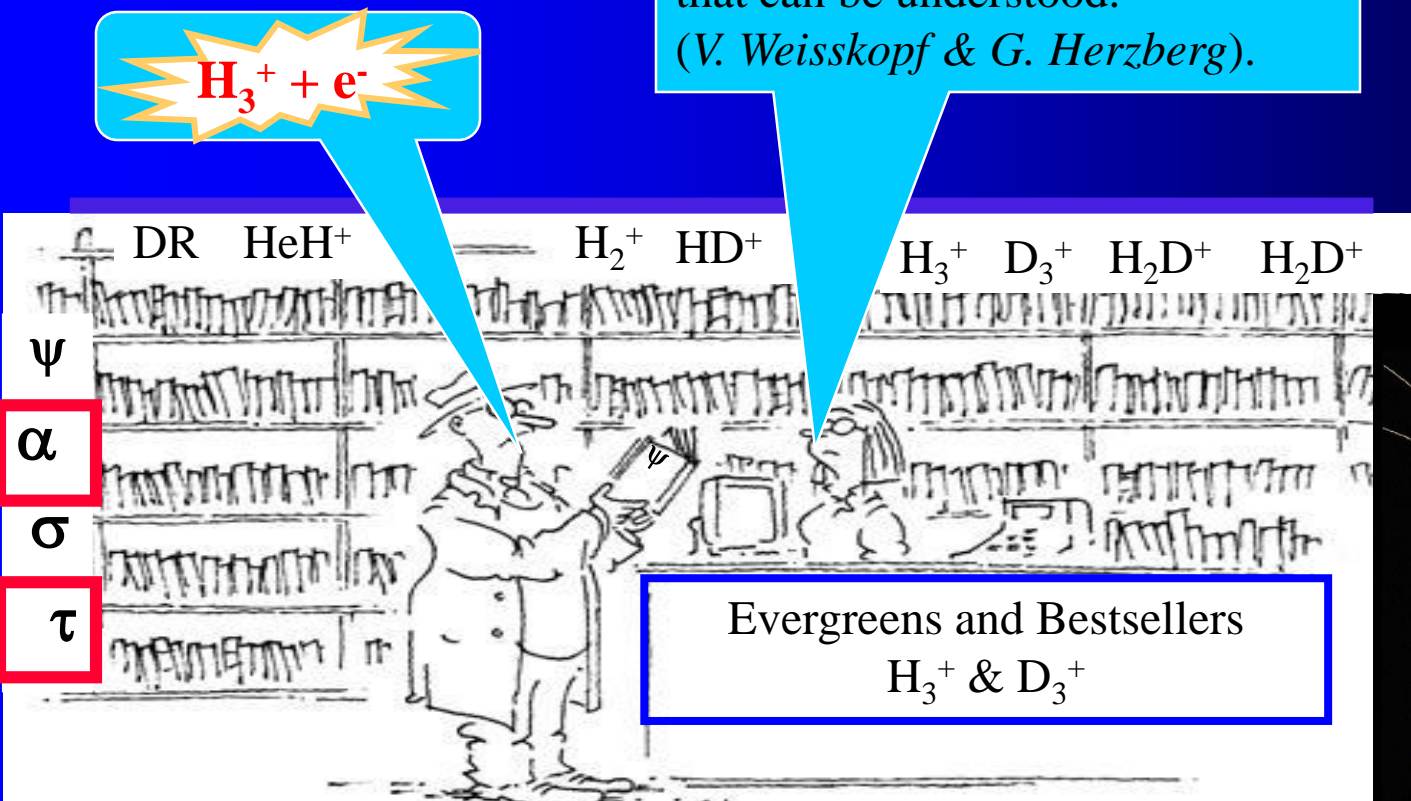
Andromeda composite

~0.005%.....D

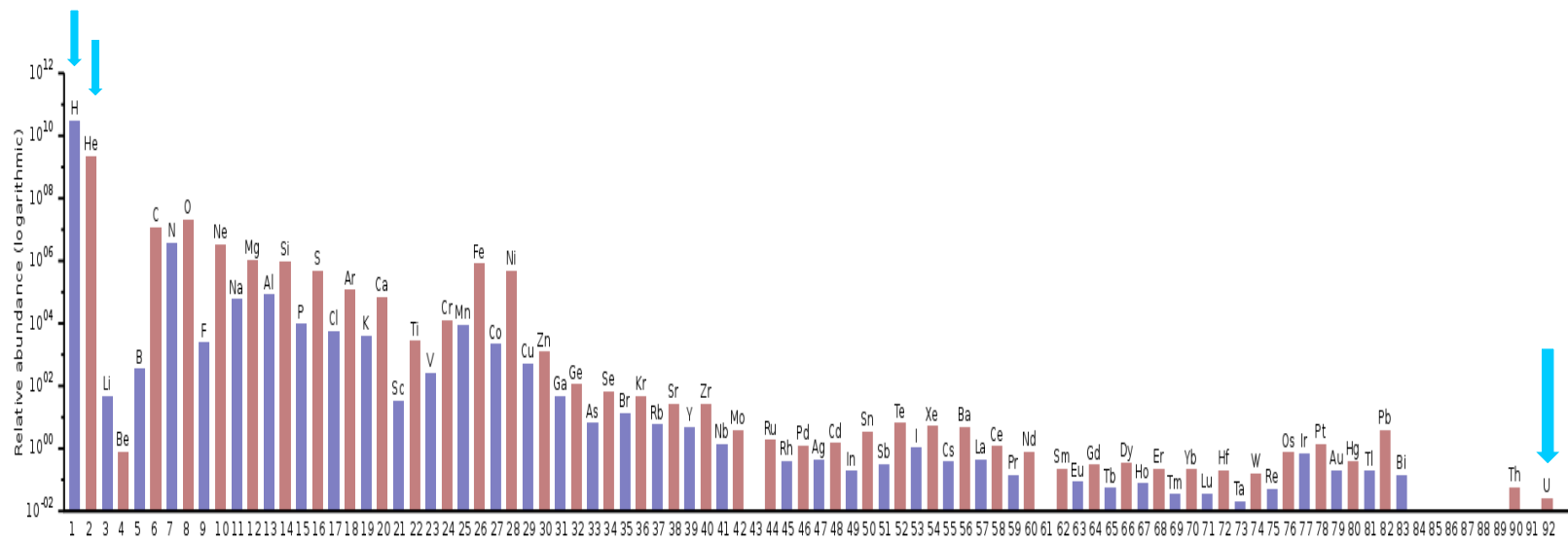
Different views
& different plasmas

H_3^+ and its interaction of with e^- is FUNDAMENTAL

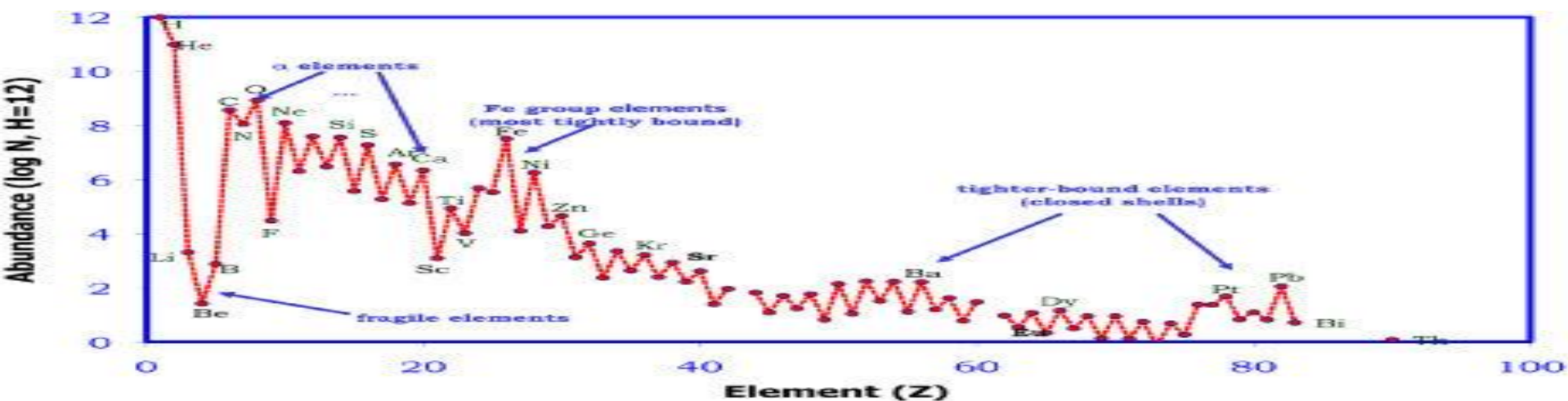
If you understand hydrogen,
you understand all
that can be understood.
(V. Weisskopf & G. Herzberg).



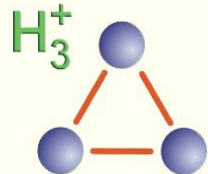
I JAKO KOMIKS.



Estimated abundances of the chemical elements in the Solar System
(logarithmic scale)



The cosmic elemental abundances extend over 12 orders of magnitude.



H_2 and H_3^+ Story



(IMR & Recombination of H_3^+)

motto

If you understand hydrogen, you understand all that can be understood. V. Weisskopf
(Taken from G. Herzberg).



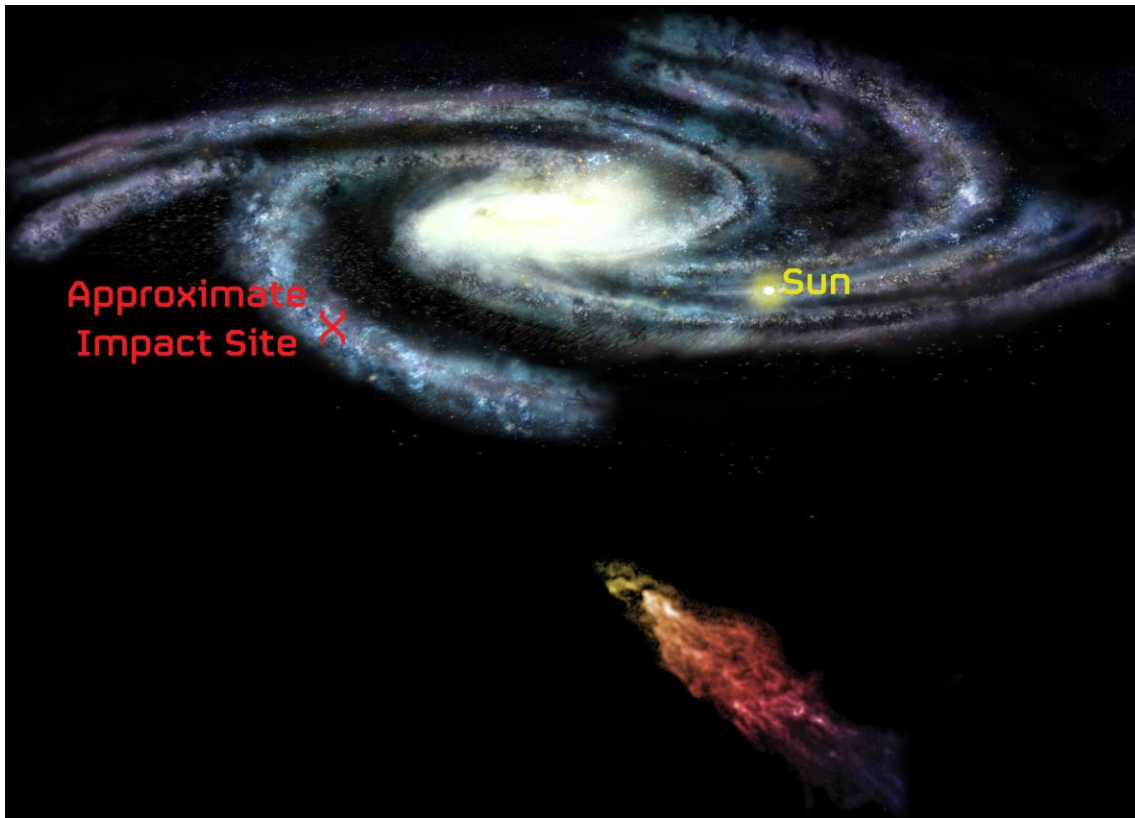
NASA/ESA/Hubble



Smith's Cloud

motivation?... \$\$\$?

called Smith's Cloud, after the astronomer who discovered it in 1963

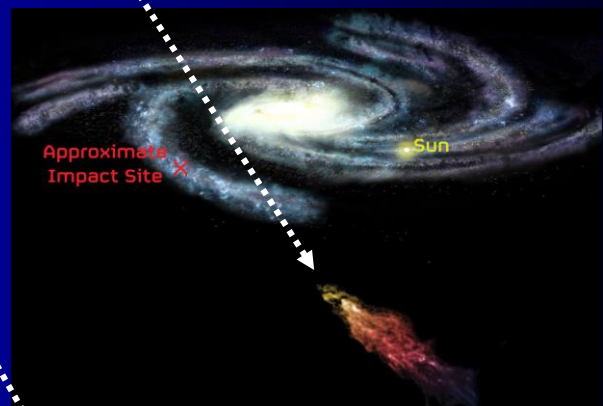


called Smith's Cloud, after the astronomer who discovered it in 1963, contains enough hydrogen to make a million stars like the Sun. Eleven thousand light-years long and 2,500 light-years wide, it is only 8,000 light-years from our Galaxy's disk. It is careening toward our Galaxy at more than 150 miles per second, aimed to strike the Milky Way's disk at an angle of about 45 degrees. Don't worry! It will hit 30,000 light years away from Earth.

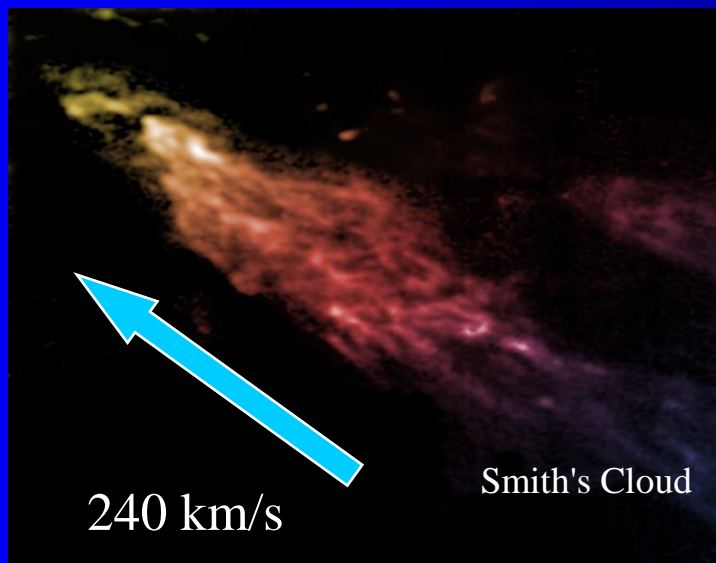
.... What about energy...

Smith's Cloud

Our Galaxy will get a rain of gas from this cloud, then in about 20 to 40 million years, the cloud's core will smash into the Milky Way's plane." The cloud will likely strike a region somewhat farther from the Galactic center than our Solar System and about 90 degrees ahead of us in the Milky Way disk. The collision may trigger a period of rapid star formation fueled by the new gas and the shock from the collision. Some theories say that the ring of bright stars near the Sun, called Gould's Belt, was created by just such a collision event.

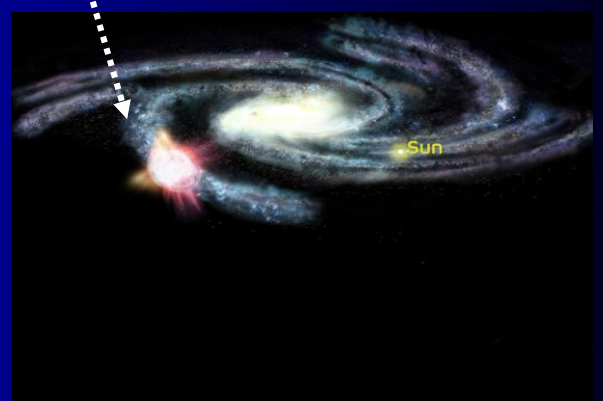
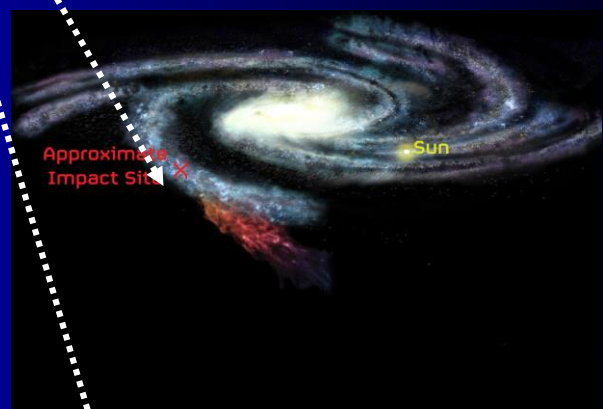


contains enough hydrogen to make a million stars like the Sun



240 km/s

240 km/s ~562 eV ~ 5×10^6 K

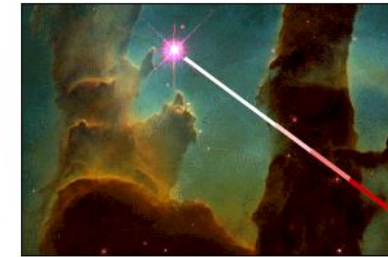


Importance of Interstellar Hydrogen

H

He

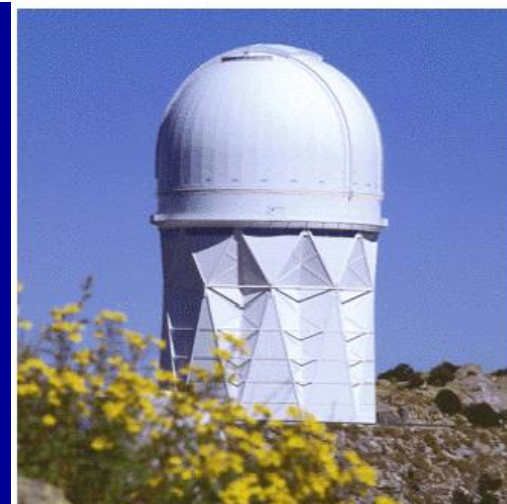
.	.	.	.
C	N	O	Ne
.	.	.	.
Mg	Si	S	Ar
Fe			



Subaru Telescope
Mauna Kea, Hawaii



Integrated area of absorption lines



Nicholas U. Mayall Telescope
Kitt Peak, AZ

United Kingdom Infrared Telescope
Mauna Kea, Hawaii

Importance of Interstellar H_3^+

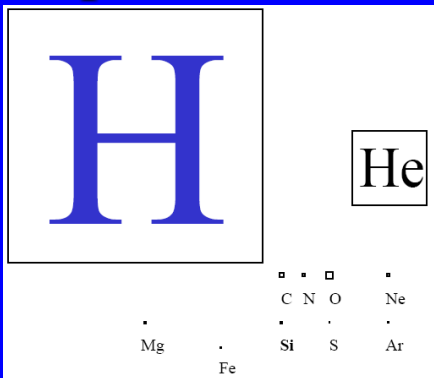
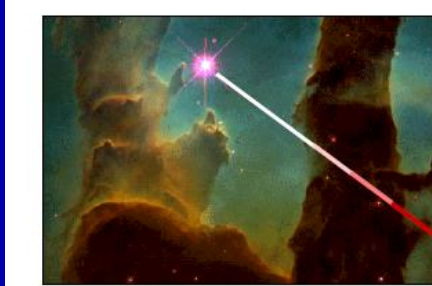
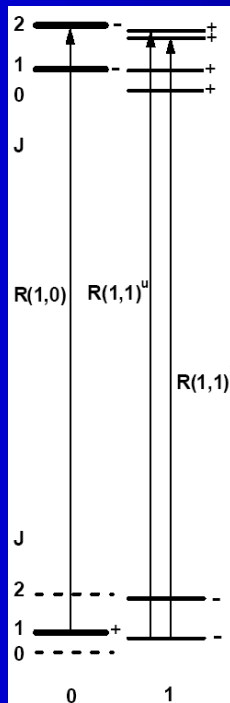


Table 2 Molecules detected in diffuse molecular clouds

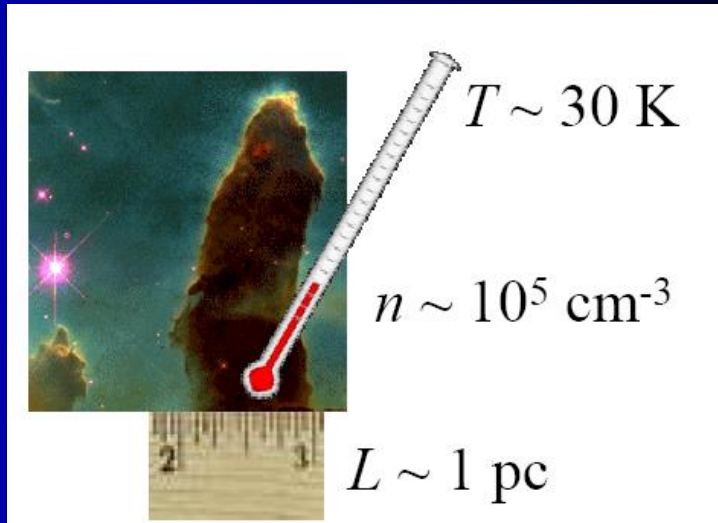
Weight	Species	Method	Target	$N(\text{X})/N_{\text{H}}$	Reference
2	H_2	UV	ζ Oph	0.56	1
3	HD	UV	ζ Oph	4.5 (-7)	2
3	H_3^+	IR	ζ Per	5.1 (-8)	3
13	CH	Optical	ζ Oph	1.5 (-9)	4
13	CH^+	Optical	ζ Oph	2.4 (-8)	5
14	$^{13}\text{CH}^+$	Optical	ζ Oph	3.5 (-10)	6
15	NH	Optical	ζ Oph	6.2 (-10)	7
17	OH	UV	ζ Oph	3.3 (-8)	8
24	C_2	Optical	ζ Oph	1.3 (-8)	9
25	C_2H	mm abs.	BL Lac	1.8 (-8)	10
26	CN	Optical	ζ Oph	1.9 (-9)	11
27	HCN	mm abs.	BL Lac	2.6 (-9)	12
27	HNC	mm abs.	BL Lac	4.4 (-10)	12
28	N_2	UV	HD 124314	3.1 (-8)	13
28	CO	UV	X Per	6.4 (-6)	14
29	HCO^+	mm abs.	BL Lac	1.5 (-9)	15
29	HO^+	mm abs.	BL Lac	2.2 (-11)	15
29	^{13}CO	UV	X Per	8.9 (-8)	16
29	C^{17}O	UV	X Per	7.4 (-10)	16
30	C^{18}O	UV	X Per	2.1 (-9)	16
30	H_2CO	mm abs.	BL Lac	3.7 (-9)	17
36	C_3	Optical	ζ Oph	1.1 (-9)	18
36	HCl	UV	ζ Oph	1.9 (-10)	19
38	C_3H_2	mm abs.	BL Lac	6.4 (-10)	10
44	CS	mm abs.	BL Lac	1.6 (-9)	20
64	SO_2	mm abs.	BL Lac	≤ 8.2 (-10)	20



Subaru Telescope
Mauna Kea, Hawaii

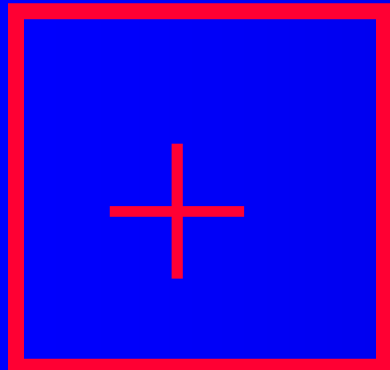


Integrated area of absorption lines

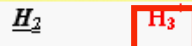


Plasma

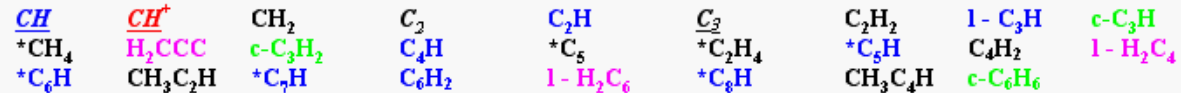
Plasma.



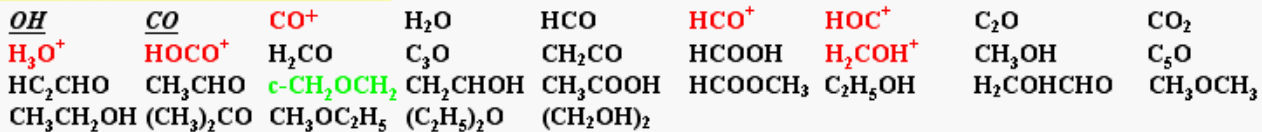
Hydrogen containing molecules



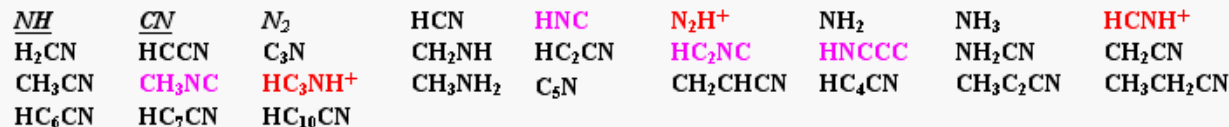
Hydrogen + carbon containing molecules



Hydrogen + oxygen + carbon containing molecules



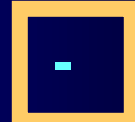
Hydrogen + nitrogen + carbon containing molecules



Hydrogen + nitrogen + oxygen + carbon containing molecules



Other species



Motivations

- H_3^+ is the cornerstone of ion-molecule reactions in the interstellar medium (ISM)
- Simple chemistry allows for the inference of various physical parameters (density, temperature, ionization rate, cloud size)

Table 1 Classification of Interstellar Cloud Types

	Diffuse Atomic	Diffuse Molecular	Translucent	Dense Molecular
Defining Characteristic	$f^n_{\text{H}_2} < 0.1$	$f^n_{\text{H}_2} > 0.1 \ f^n_{\text{C}+} > 0.5$	$f^n_{\text{C}+} < 0.5 \ f^n_{\text{CO}} < 0.9$	$f^n_{\text{CO}} > 0.9$
A_V (min.)	0	~ 0.2	$\sim 1\text{--}2$	$\sim 5\text{--}10$
Typ. n_{H} (cm^{-3})	10–100	100–500	500–5000?	$> 10^4$
Typ. T (K)	30–100	30–100	15–50?	10–50
Observational Techniques	UV/Vis HI 21-cm	UV/Vis IR abs mm abs	Vis (UV?) IR abs mm abs/cm	IR abs mm cm



The Orion molecular clouds

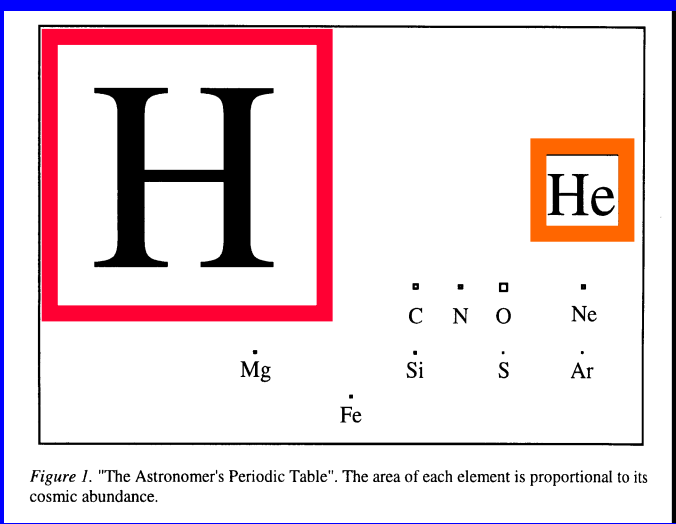
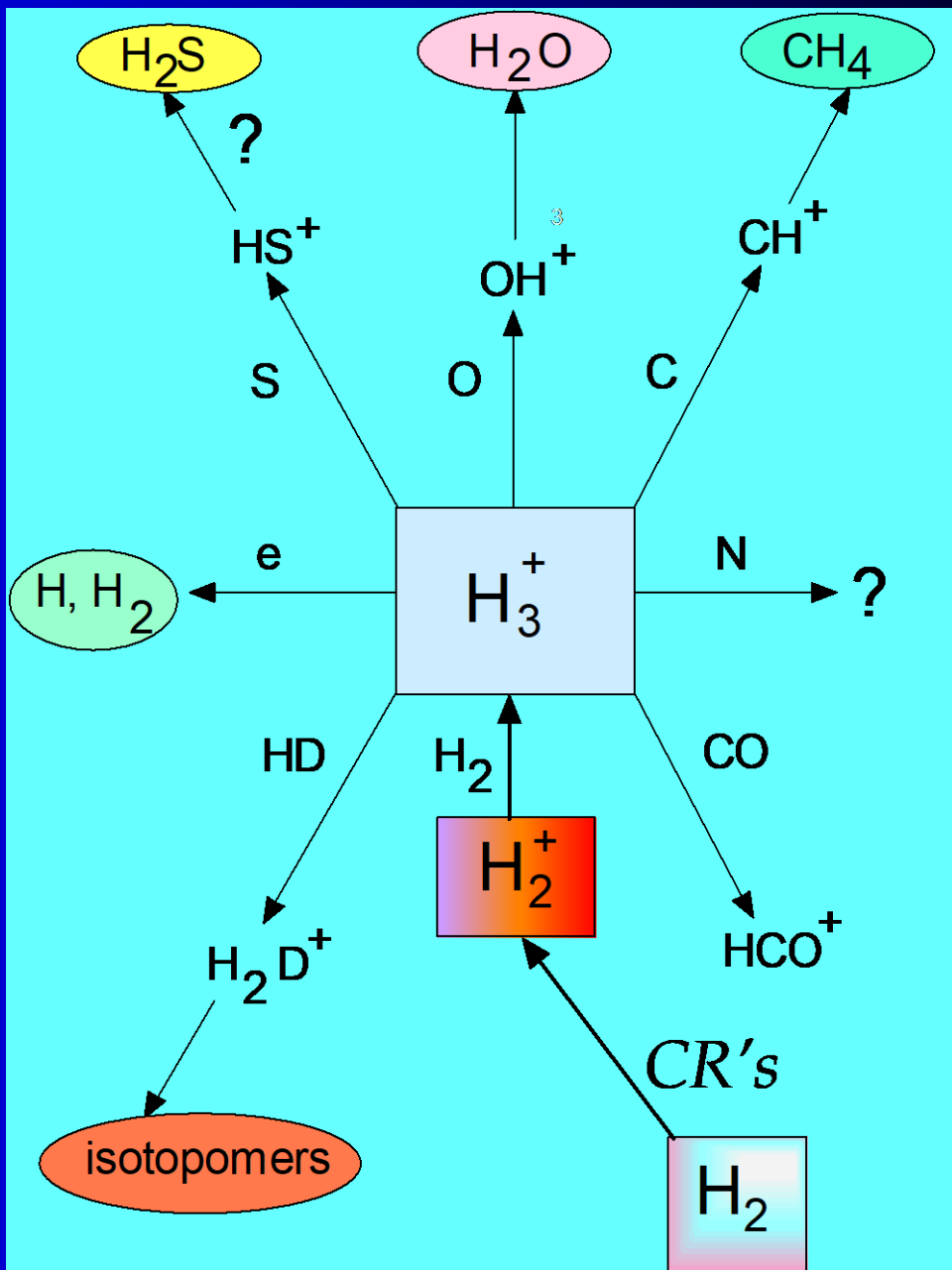


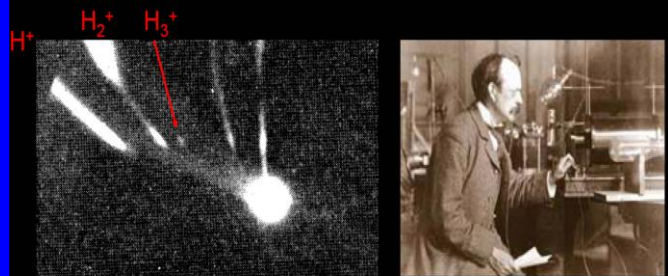
Figure 1. "The Astronomer's Periodic Table". The area of each element is proportional to its cosmic abundance.



History of H₃⁺

J. J. Thomson

1912

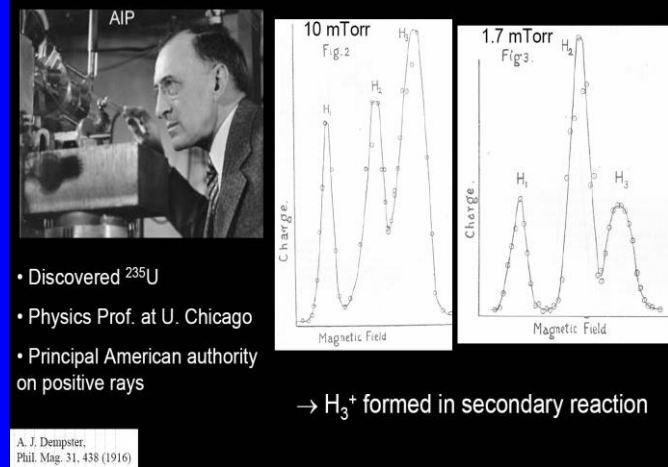


Existence of H₃.—On several plates taken when the discharge-tube contains hydrogen, the existence of a primary line for which $m/e = 3$ has been detected. There can, I think, be little doubt that this line is due to H₃. The existence of this substance is interesting from a chemical point of view, as it is not possible to reconcile its existence with the ordinary conceptions about valency, if hydrogen is regarded as always monovalent. The polymeric modification of hydrogen seems to require special conditions for its formation, for it cannot be detected on many of the plates taken with hydrogen in the tube.

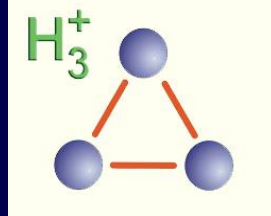
J. J. Thomson.
Phil. Mag. 24, 209 (1912)

m=3

Arthur J. Dempster 1916



1935 Charles A. Coulson



- First Ph.D. student of Lennard-Jones
- First ab initio calculation on a polyatomic molecule
- "It appears that the ion H₃⁺ should exist in stable equilateral form with a nuclear distance about 0.85 Å, and that all excited levels are unstable."
- Prediction not accepted by Eyring, Hirschfelder, and others
- With advent of computers, prediction was confirmed (Christoffersen, Hagstrom, & Prosser 1964, Conroy 1964)

C. A. Coulson.
Proc. Camb. Phil. Soc. 31, 244 (1935)



- No excited electronic state
- No dipole moment in ground state
– → no pure rotational spectrum
- ν_1 symmetric stretch - infrared inactive
- ν_2 vibration fundamental band feasible freq. $\sim 2700 \text{ cm}^{-1}$

Intensive laboratory search for H₃⁺ spectra

1912 1920 1930 1970 1980



H_3^+ in Interstellar space

Interstellar H_3^+

1961

ON THE POSSIBLE OCCURRENCE OF H_3^+ IN INTERSTELLAR SPACE

The possibilities for detection of the molecular ion H_2^+ by radio-astronomical techniques have recently received considerable attention, and theoretical predictions of the spectrum have been made by Mizushima (1961) and by Burke (1961). Recent work on ion-molecule reactions indicates that the molecular ion H_3^+ may also be expected in interstellar space. In fact, with the presence of quantities of molecular hydrogen, H_2^+ will react to form H_3^+ .

Formation of H_3^+ through the reaction $H_2^+ + H_2 \rightarrow H_3^+$ has been observed independently by Stevenson and Schissler (1958) and by Barnes, Martin, and McDaniel (1961). The cross-section for this reaction has been found to have a remarkably large value of the order of 10^{-14} cm^2 at normal thermal energies. This is much greater than the gas-kinetic cross-section for neutral hydrogen molecules. The cross-section for H_3^+ formation by this reaction varies inversely with the relative velocity of the H_2^+ ion and the hydrogen molecule (Stevenson and Schissler 1958; Lampe and Field 1959). The experimental work of Barnes, Martin, and McDaniel furthermore shows that H_3^+ ions persist over very many subsequent collisions with hydrogen molecules. The H_3^+ ion is stable against spontaneous dissociation. Its binding energy of 4.18 ev (Varney 1960) exceeds that of H_2^+ (2.65 ev), so the formation reaction is exoergic (Hirschfelder, Curtiss, and Bird 1954).

Thus it may be expected that H_2^+ will be converted to H_3^+ upon encounter with a hydrogen molecule, and the population of H_3^+ will be very strongly influenced by the density of neutral molecular hydrogen. It now appears desirable to consider the possibilities for detecting H_3^+ because this molecular ion may be present under some circumstances to the virtual exclusion of H_2^+ .

D. W. MARTIN
E. W. McDANIEL
M. L. MEEKS

June 13, 1961

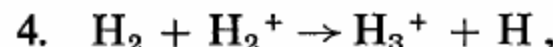
GEORGIA INSTITUTE OF TECHNOLOGY
ATLANTA, GEORGIA

Martin, McDaniel, & Meeks,
Astrophys. J. 134, 1012 (1961)

Interstellar Chemistry

1973

Another important subclass of reactions are those involving H_3^+ . This ion is produced by the well-studied reaction



and then reacts with many neutral species according to the general formula



where $X = CO, N_2, H_2O, NH_3$, etc. These reactions have been studied by Burt *et al.*

E. Herbst & W. Klemperer,
Astrophys. J. 185, 505 (1973)

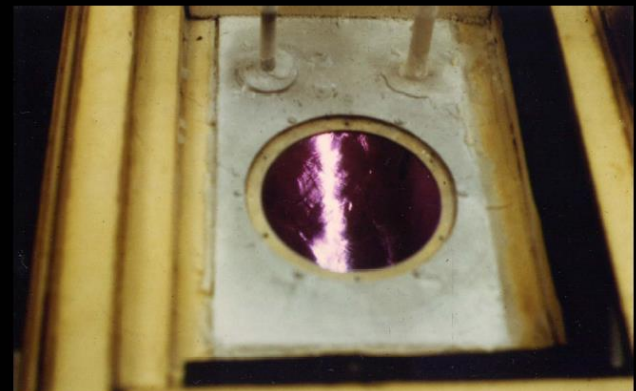
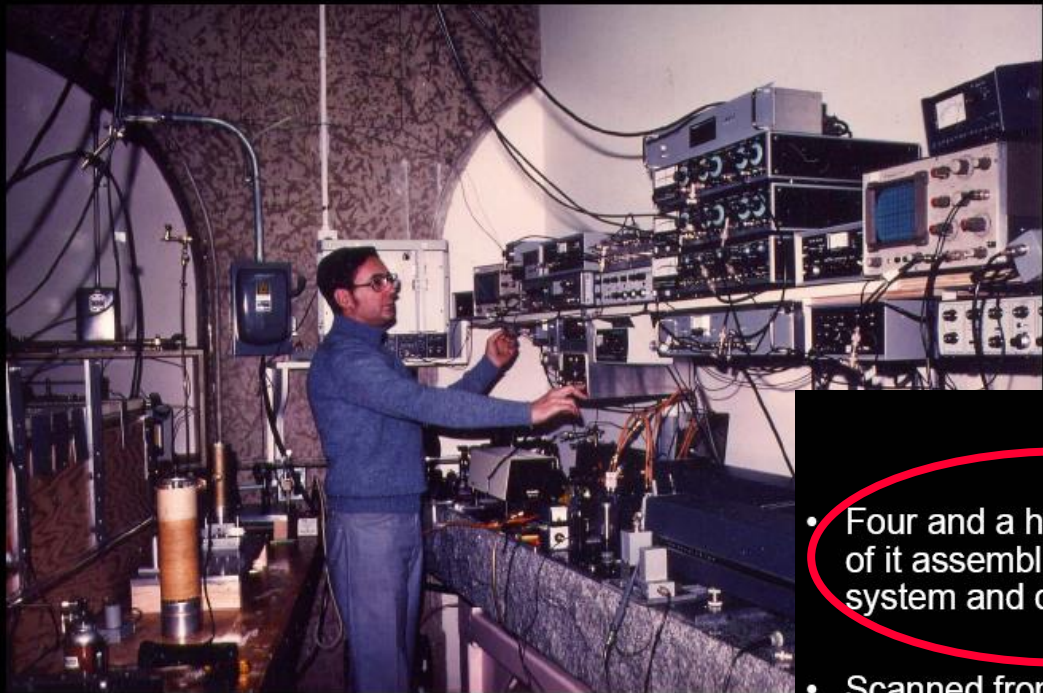
also: W. D. Watson
Astrophys. J. 183, L17 (1973)

- H_3^+ “universal protonator”
 - $H_3^+ + O \rightarrow H_2 + OH^+$
 - $OH^+ + H_2 \rightarrow H + H_2O^+$
 - $H_2O^+ + H_2 \rightarrow H + H_3O^+$
 - $H_3O^+ + e^- \rightarrow H_2O + H$
- Origin of Earth's water (?)

Search for H₃⁺ in laboratory

Oka's Search for H₃⁺

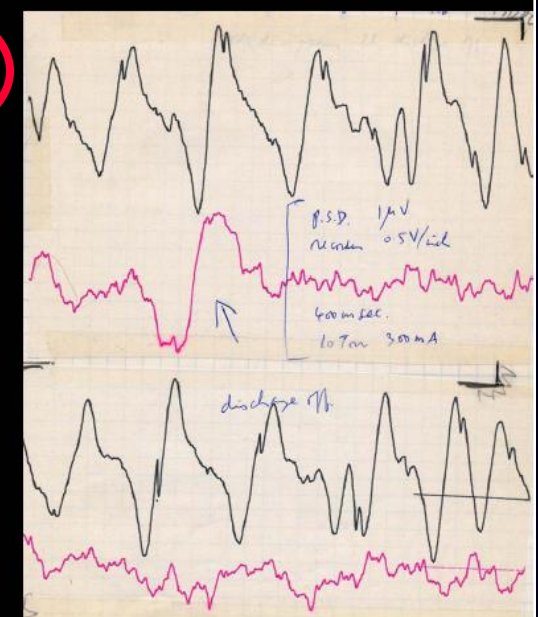
Positive Column Discharge



Every morning, he transferred six 50 liter cans of liquid nitrogen to the laboratory!

The Long Search

- Four and a half years. Much of it assembling the DF system and discharge cell.
- Scanned from:
 - 6/12-8/3 (1978)
 - 12/18-1/26 (1978-79)
 - 4/24-12/18 (1980)
- R(1,0) April 25, 1980.
 - Oka and Allen Karabonik in lab
 - Keiko came in at 10 pm
- Watson assigned it overnight



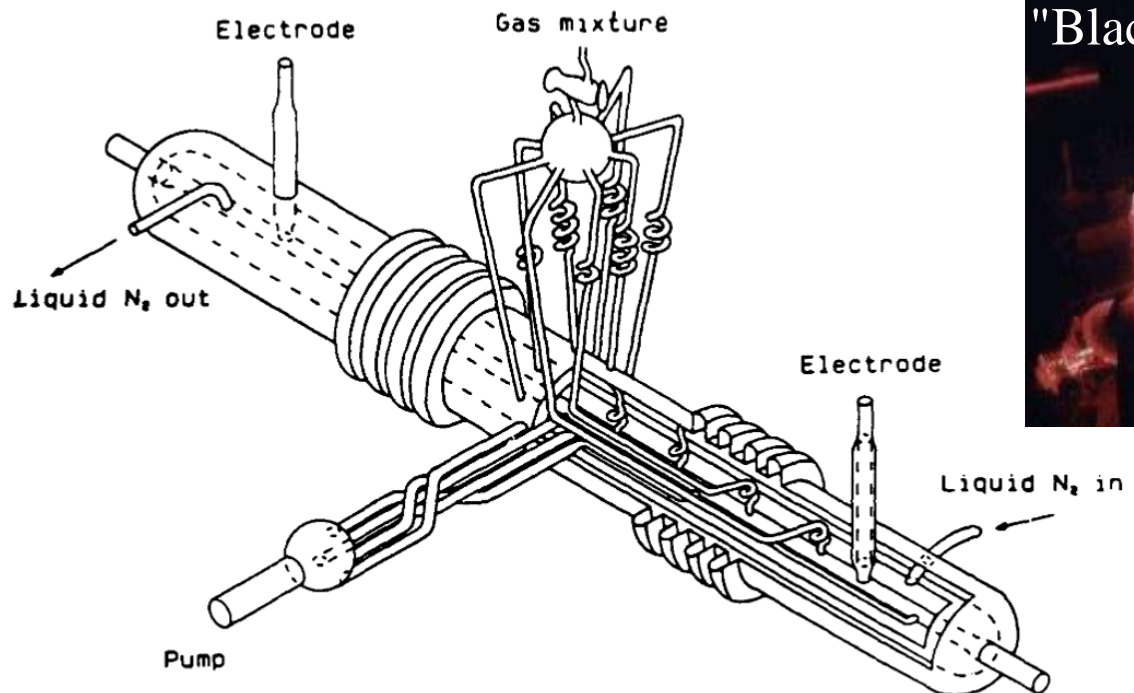


Fig. 8. The multiple inlet-outlet liquid nitrogen cooled plasma tube (nicknamed "Black Widow").

Aastrophysical – Observations of $\text{H}_3^+ (v=0)$

1912 .. 1916 ... 1935

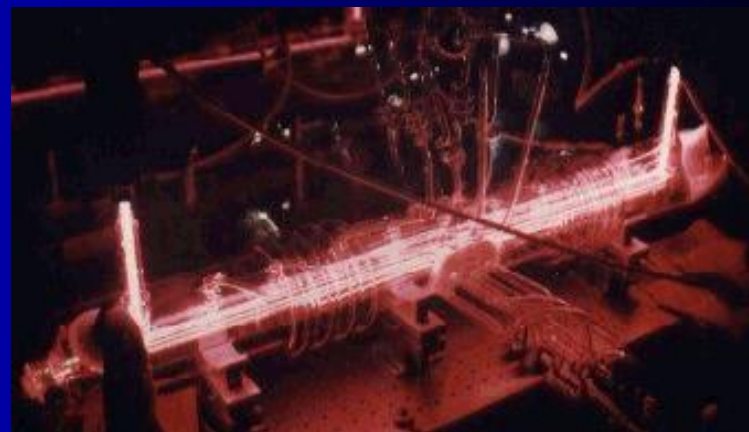
1980

"Black Widow"

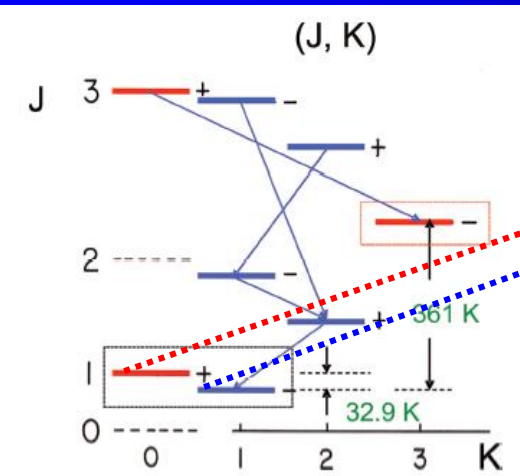
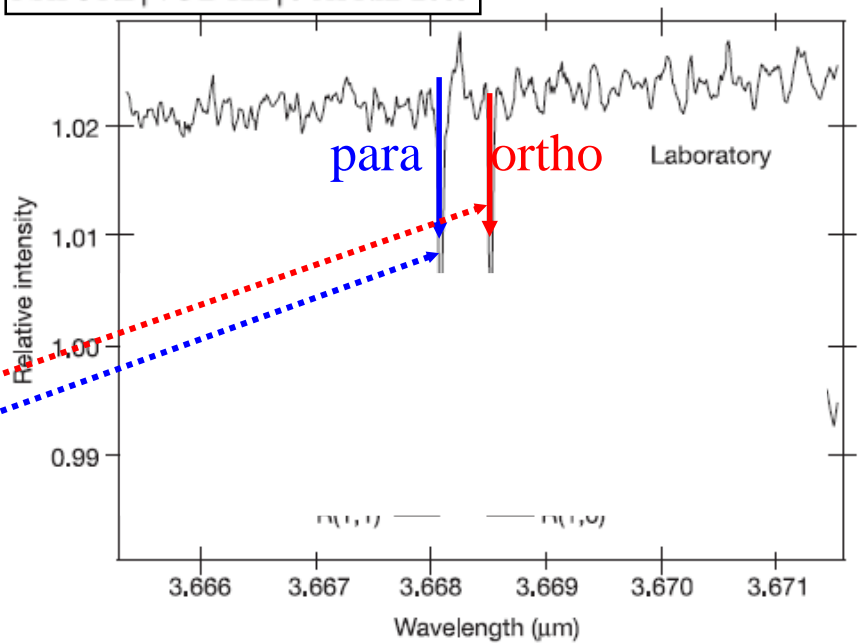
1980 - Laboratory

T. Oka -IR Spectroscopy Observation of H_3^+

Oka, T. 1980 *Phys. Rev. Lett.* 45, 531.

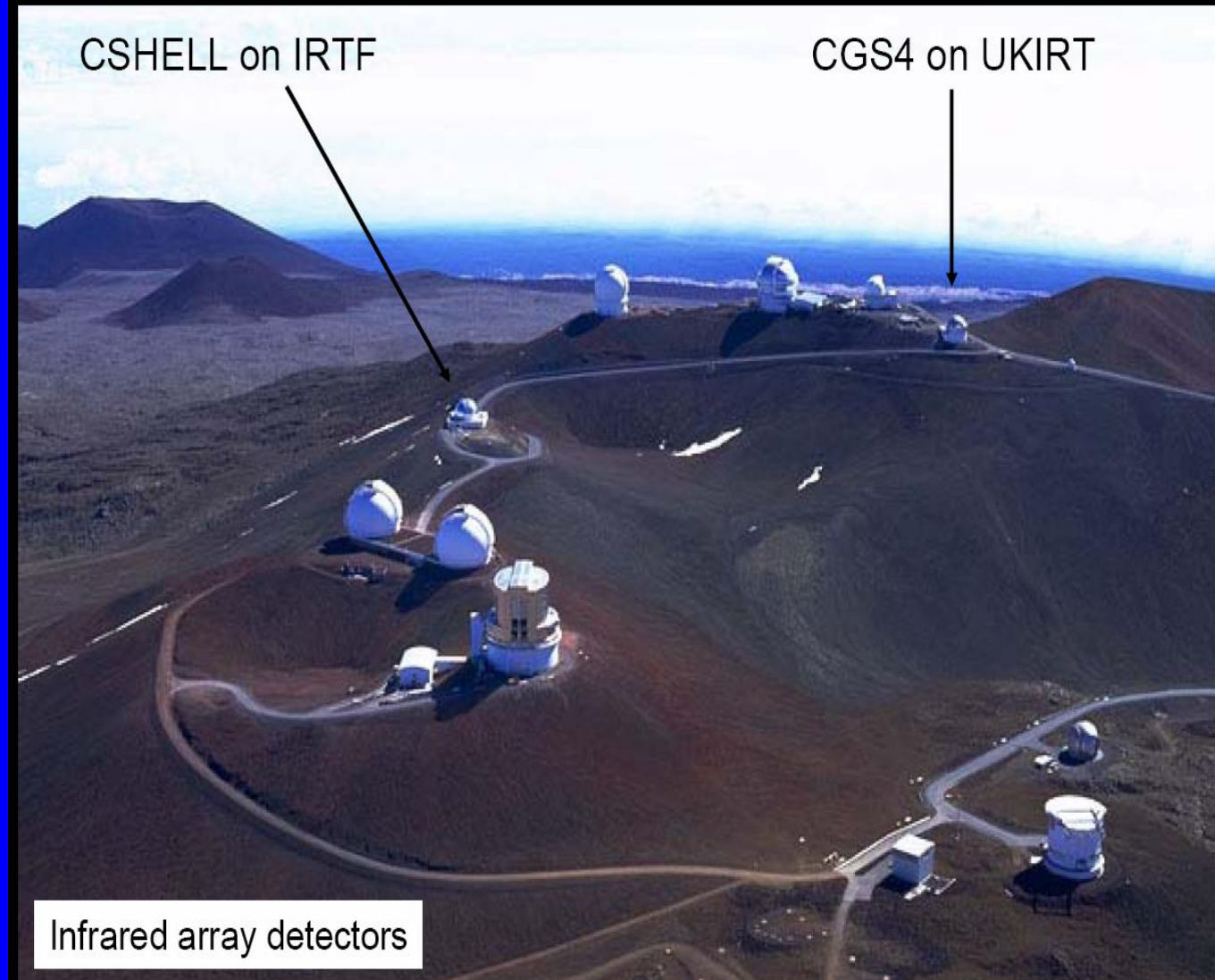


NATURE | VOL 422 | 3 APRIL 2003



R(1,1)u originates from the lowest para level ($J = 1, K = 1$), while R(1,0) comes from the lowest ortho level ($J = 1, K = 0$). Note that the ($J = K = 0$) level is forbidden by the Pauli principle.

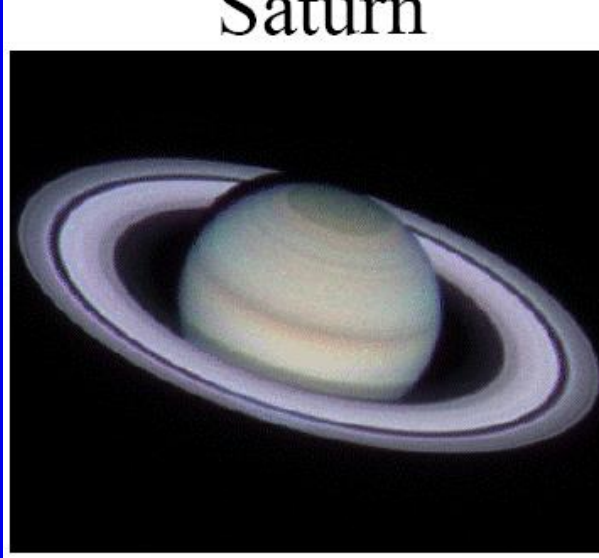
Back to the Interstellar Search



Jupiter

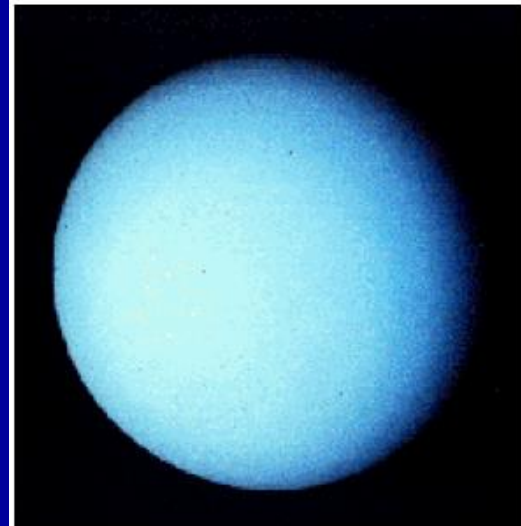


Saturn



Environments with H_3^+

Uranus



Observation of H_3^+ : **1987-1993**

Ionosphere of large planets:

**Jupiter (1987), Saturn (1993),
Uran(1993)**

Search for H₃⁺ - Interstellar space

First detection!

LETTERS TO NATURE

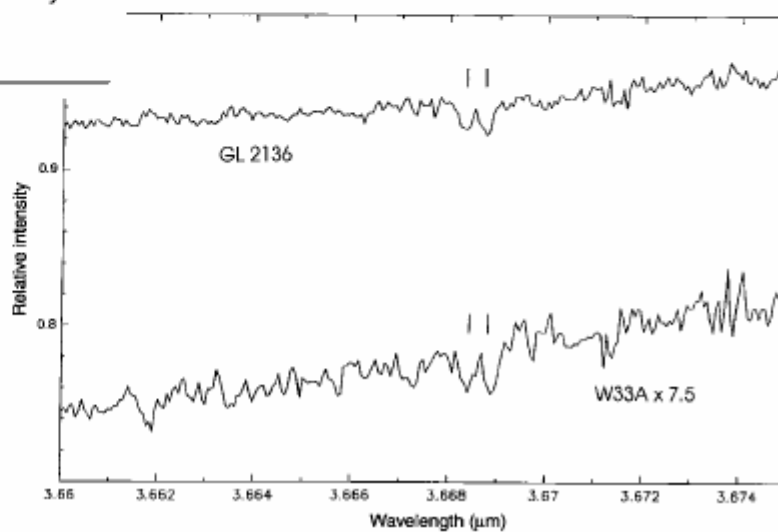
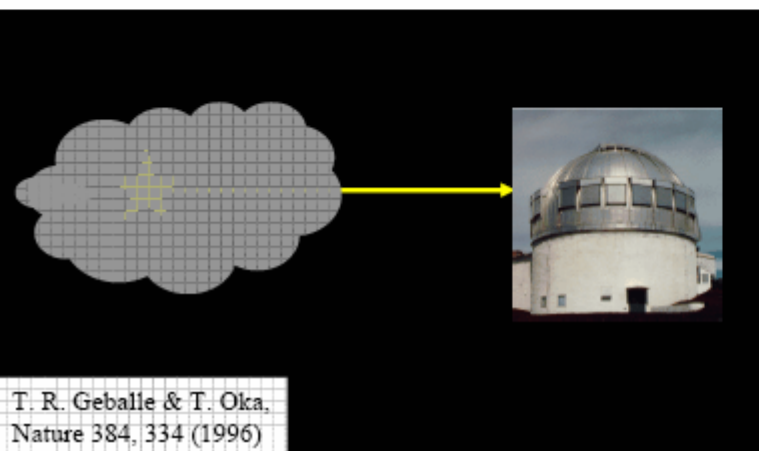
1996

Detection of H₃⁺ in interstellar space

T. R. Geballe* & T. Oka†

* Joint Astronomy Centre, University Park, Hilo, Hawaii 96720, USA

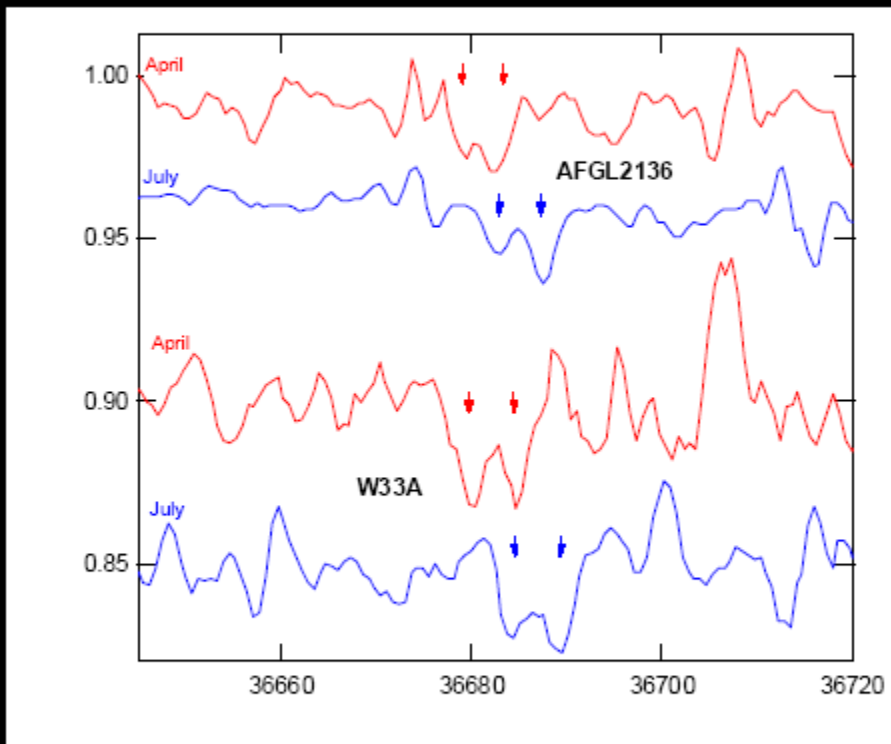
† Department of Astronomy and Astrophysics, Department of Chemistry and the Enrico Fermi Institute, The University of Chicago, Chicago, Illinois 60637-1403, USA



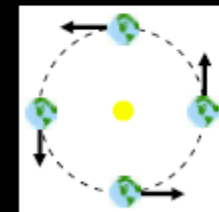
Search for H₃⁺ - Interstellar space

Confirmed by Doppler Shift

1996

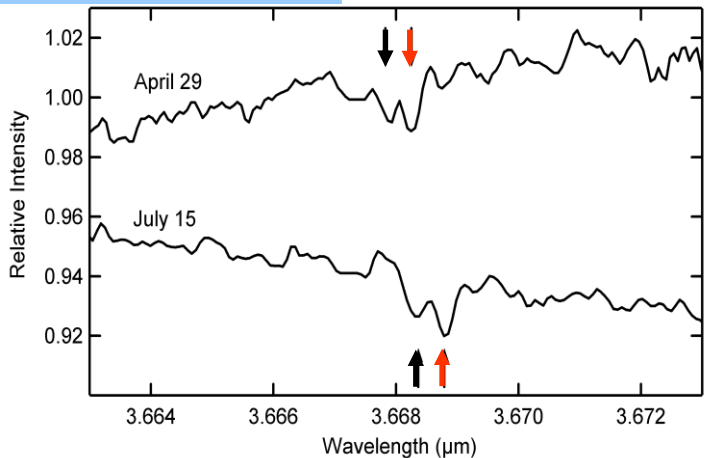


reprocessed
↓
Doppler shift
confirms
interstellar
origin



Conditions in ISM

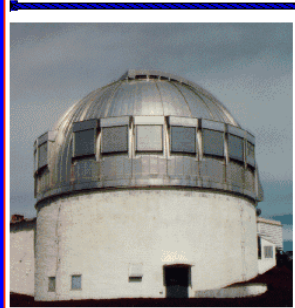
T. R. Geballe & T. Oka
Nature 384, 334 (1996)



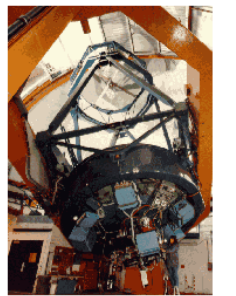
$$N_{\text{para}} = 4.0(9) \times 10^{14} \text{ cm}^{-2}$$

$$N_{\text{ortho}} = 3.0(6) \times 10^{14} \text{ cm}^{-2} (\Delta E \sim 32.9 \text{ K})$$

Molecular Cloud GL2136.
The first detection of interstellar H_3^+
CGS4 spectrometer at UKIRT



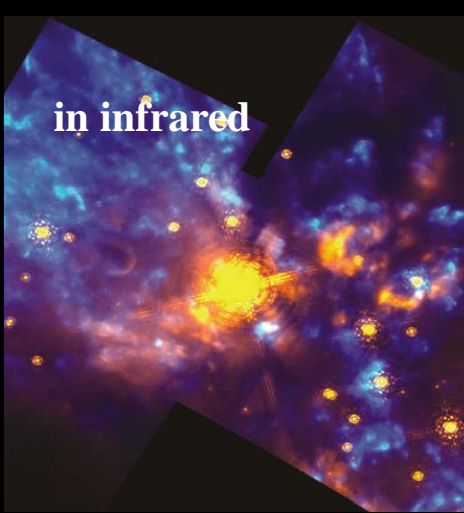
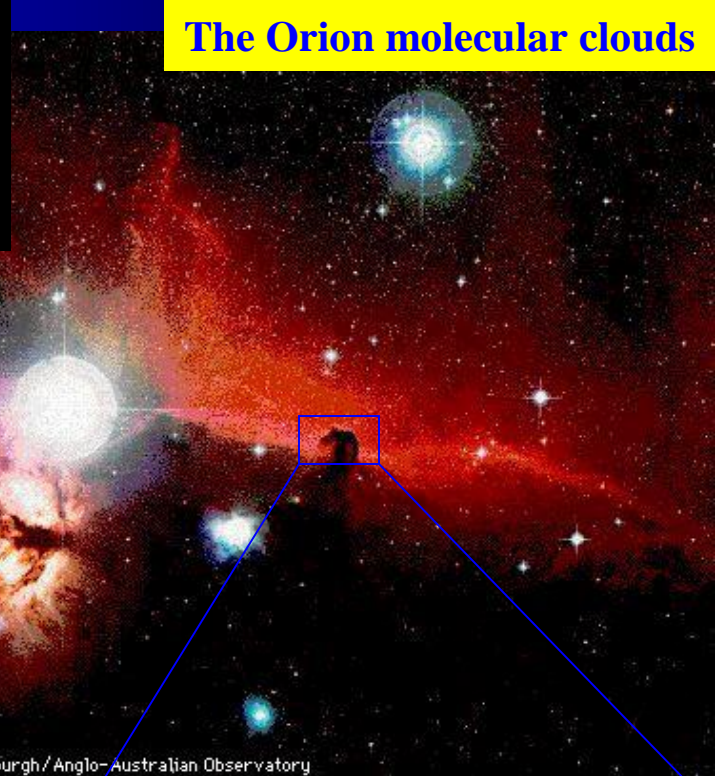
United
Kingdom
Infrared
Telescope
(UKIRT)

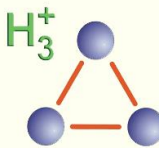


Dark Clouds:

- $T \sim 10\text{K}$
- H_2 density $\sim 10^4 \text{ cm}^{-3}$

The Orion molecular clouds



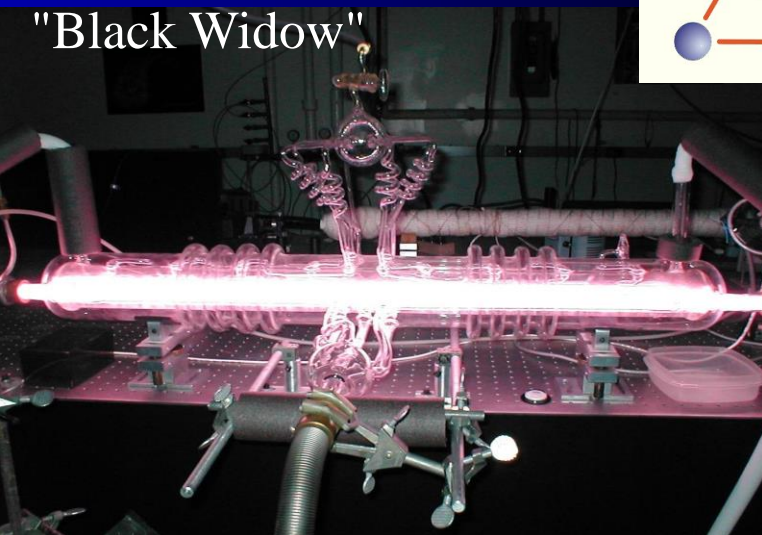


Astrophysical – Observations OF H_3^+ (v=0)

1980 - Laboratory

T. Oka -IR Spectroscopy Observation of H_3^+

Oka, T. 1980 *Phys. Rev. Lett.* 45, 531.



1987 -2006; Observation of H_3^+ :

Supernova 1987A

Interstellar clouds (1998....)

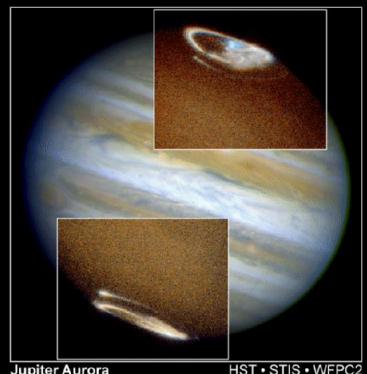
Centre of Galaxy (1999)

Ionosphere of large planets:

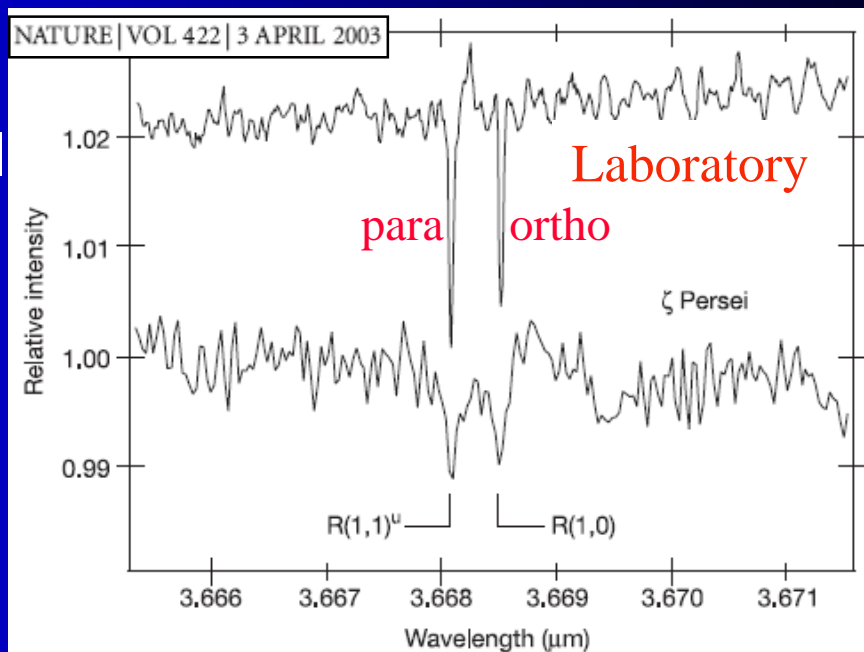
Jupiter (1987), Saturn (1993),
Uran(1993)

Geballe, T. R. & Oka, T. 1996 *Nature* 384, 334.

Jupiter



Saturn

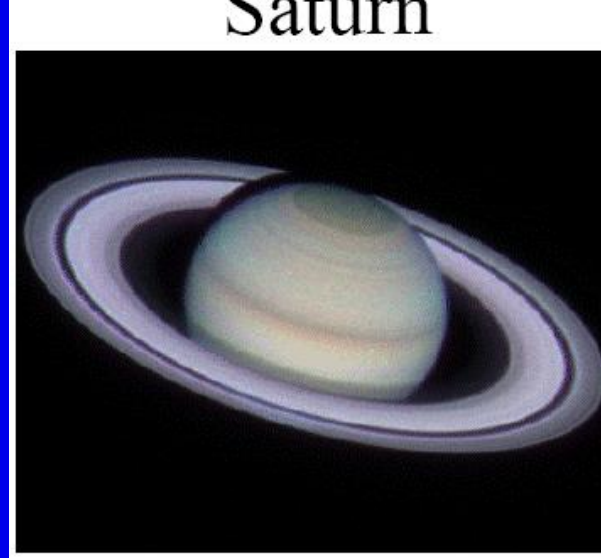


R(1,1)u originates from the lowest para level ($J = 1, K = 1$), while R(1,0) comes from the lowest ortho level ($J = 1, K = 0$). Note that the ($J = K = 0$) level is forbidden by the Pauli principle.

Jupiter



Saturn



Environments with H₃+

Uranus



Dense Clouds



Barnard 68 (João Alves)

Diffuse Clouds



Cygnus OB2 (POSS)

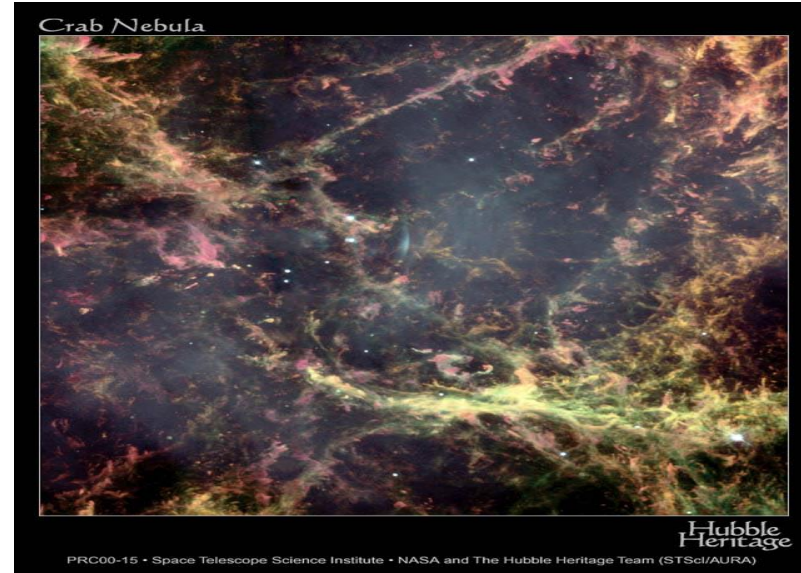
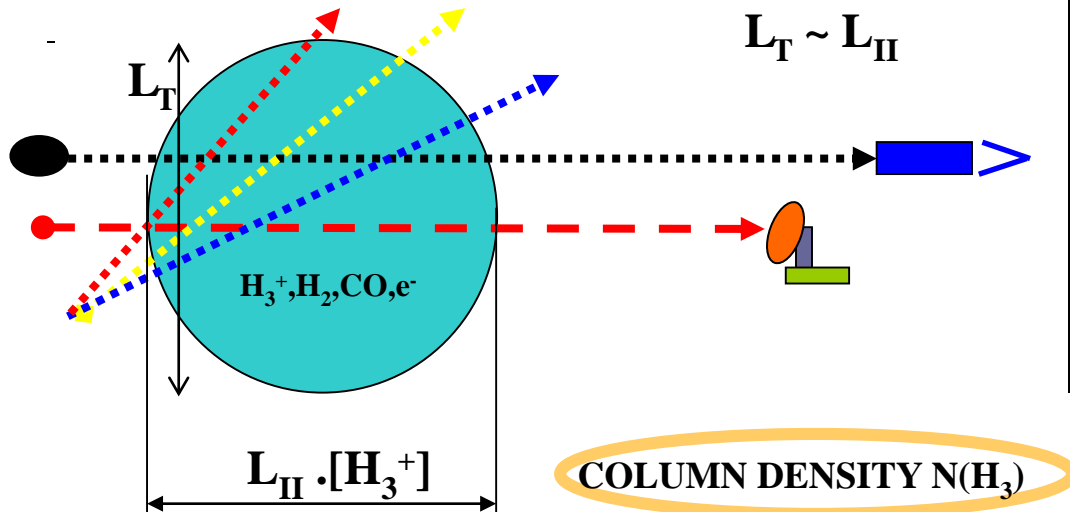
Galactic Center



Galactic Center (2MASS/MSX)

Balance in ISM

Cosmic-ray ionisation rate $\gamma \sim 3 \times 10^{-17} \text{ s}^{-1}$



PRC00-15 • Space Telescope Science Institute • NASA and The Hubble Heritage Team (STScI/AURA)



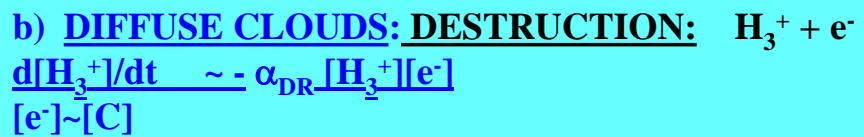
a) DENSE CLOUDS: DESTRUCTION:



$$d[H_3^+]/dt \sim -k_{CO} \cdot [H_3^+] \cdot [CO]$$

$$[H_3^+] = \gamma / k_{CO} \cdot [H_2] / [CO] = \sim 1 \times 10^{-4} \text{ cm}^{-3}$$

OK with observation



$$\alpha_{DR} = 2 \times 10^{-7} \text{ cm}^3 \text{s}^{-1} \times (T/300)^{-0.65} ?$$

$$[H_3^+] = \gamma / \alpha_{DR} \cdot [H_2] / [C] = \sim 1 \times 10^{-7} \text{ cm}^{-3}$$

NO with observation

Interstellar medium

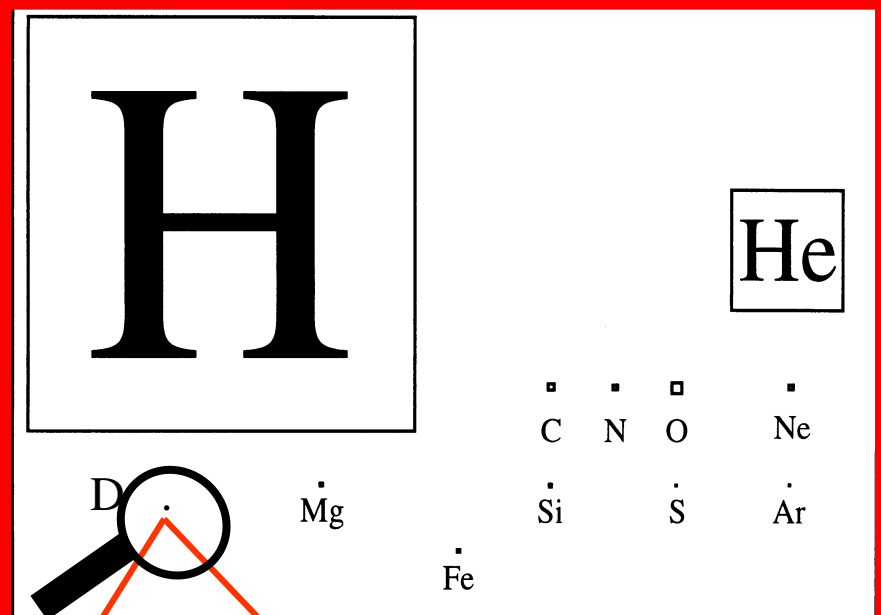
@ 10-50K

92.1% of nucleons in the universe are protons

7.8% are helium nuclei !

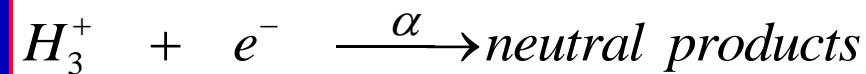
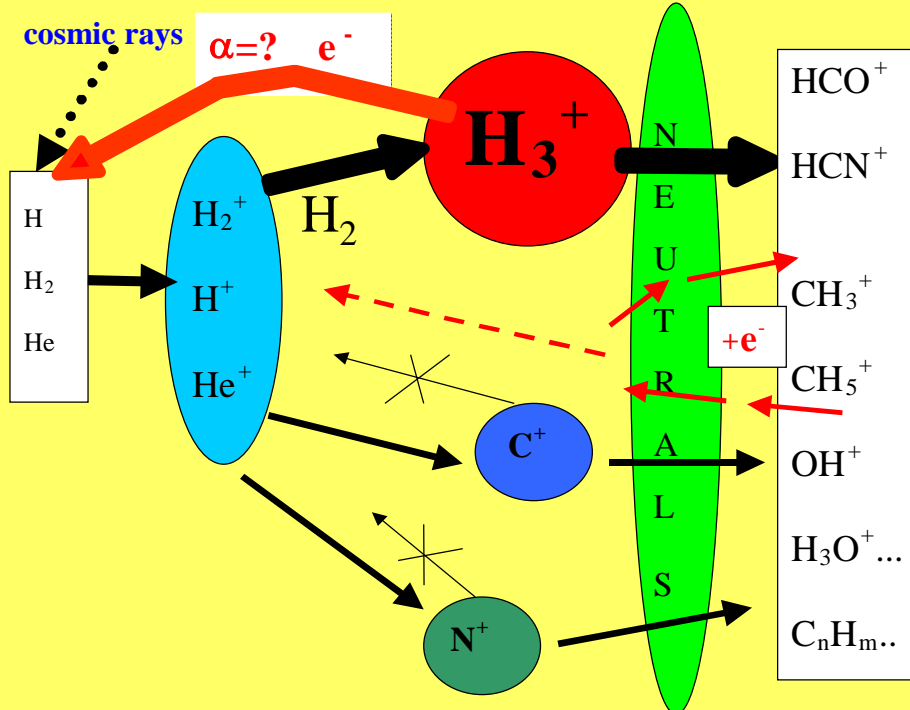
0.1%.....C,N,O,S,Si....

Cosmic abundance



D/H ratio $\sim 10^{-5}$

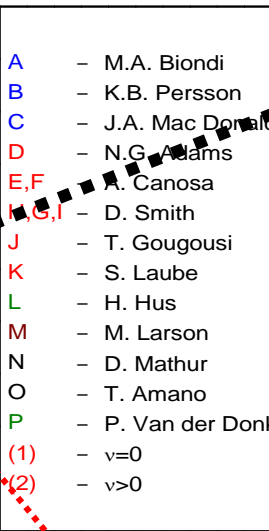
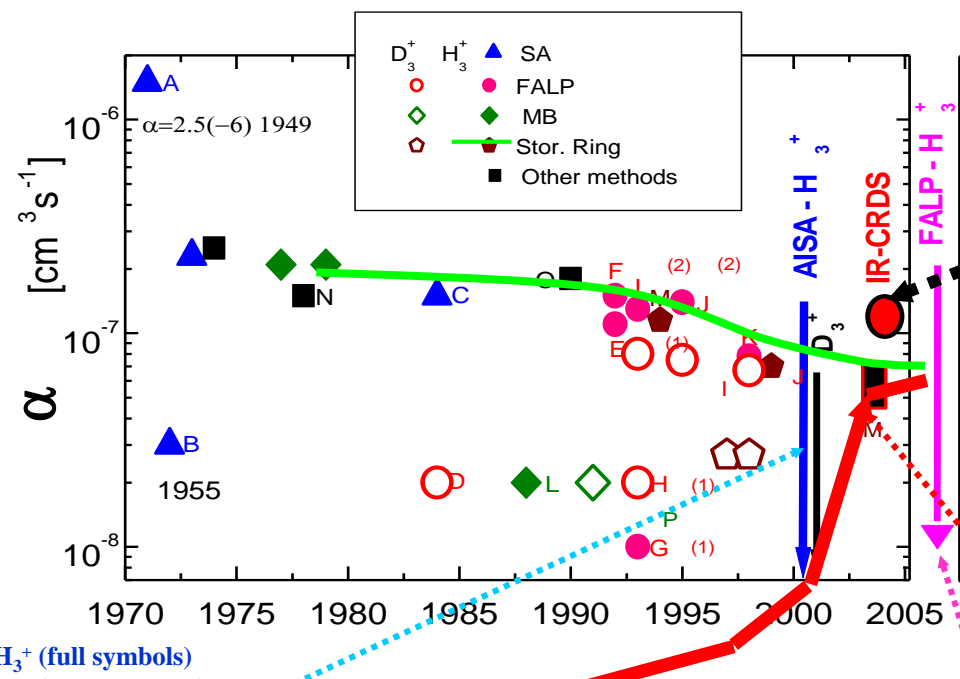
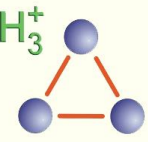
DENSE INTERSTELLAR CLOUDS



$$\alpha (10 \text{ K}) = ????$$

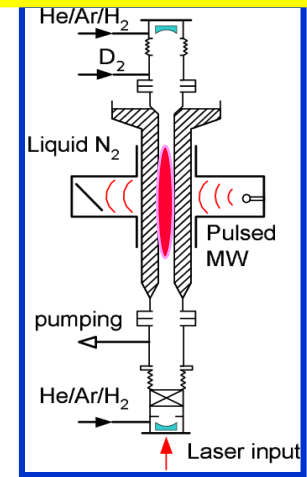
Emotional history of experiments

–“time evolution“ of $\alpha(\text{H}_3^+)$, $\alpha(\text{D}_3^+)$



CRDS

μw discharge cell



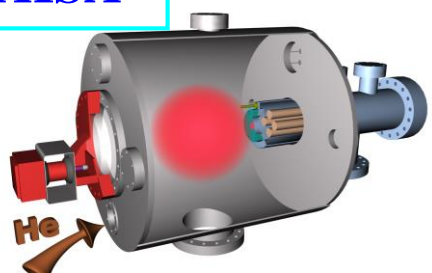
IR spectroscopy

PHYSICAL REVIEW A 68, 012703 (2003)

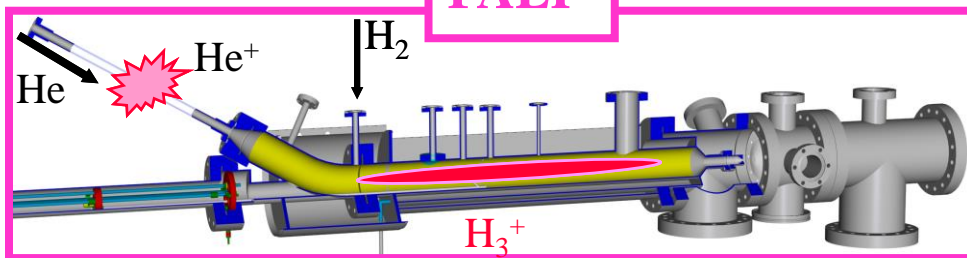
Unified theoretical treatment of dissociative recombination of D_{3h} triatomic ions:
Application to H_3^+ and D_3^+

Viatcheslav Kokouline and Chris H. Greene

AISA



FALP



Interstellar medium, HD role

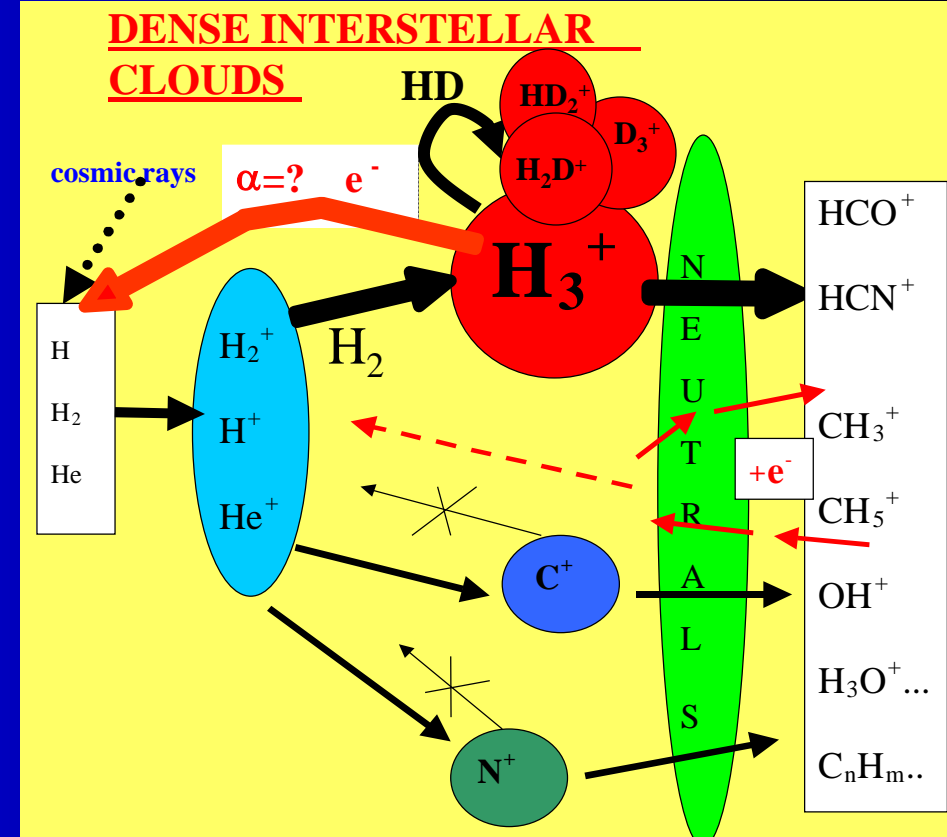
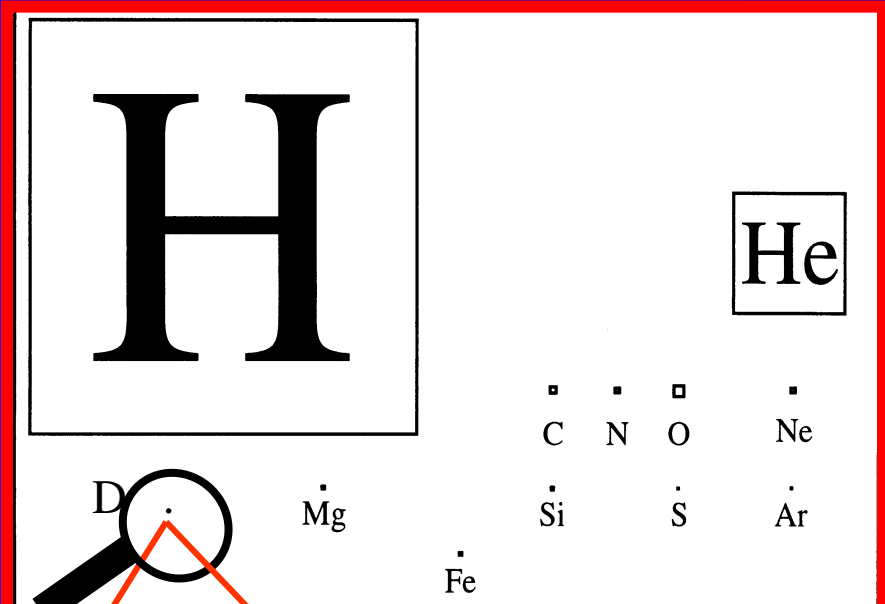
@ 10-50K

92.1% of nucleons in the universe are protons

7.8% are helium nuclei !

0.1%.....C,N,O,S,Si....

Cosmic abundance



$$\alpha (10 \text{ K}) = \text{????}$$

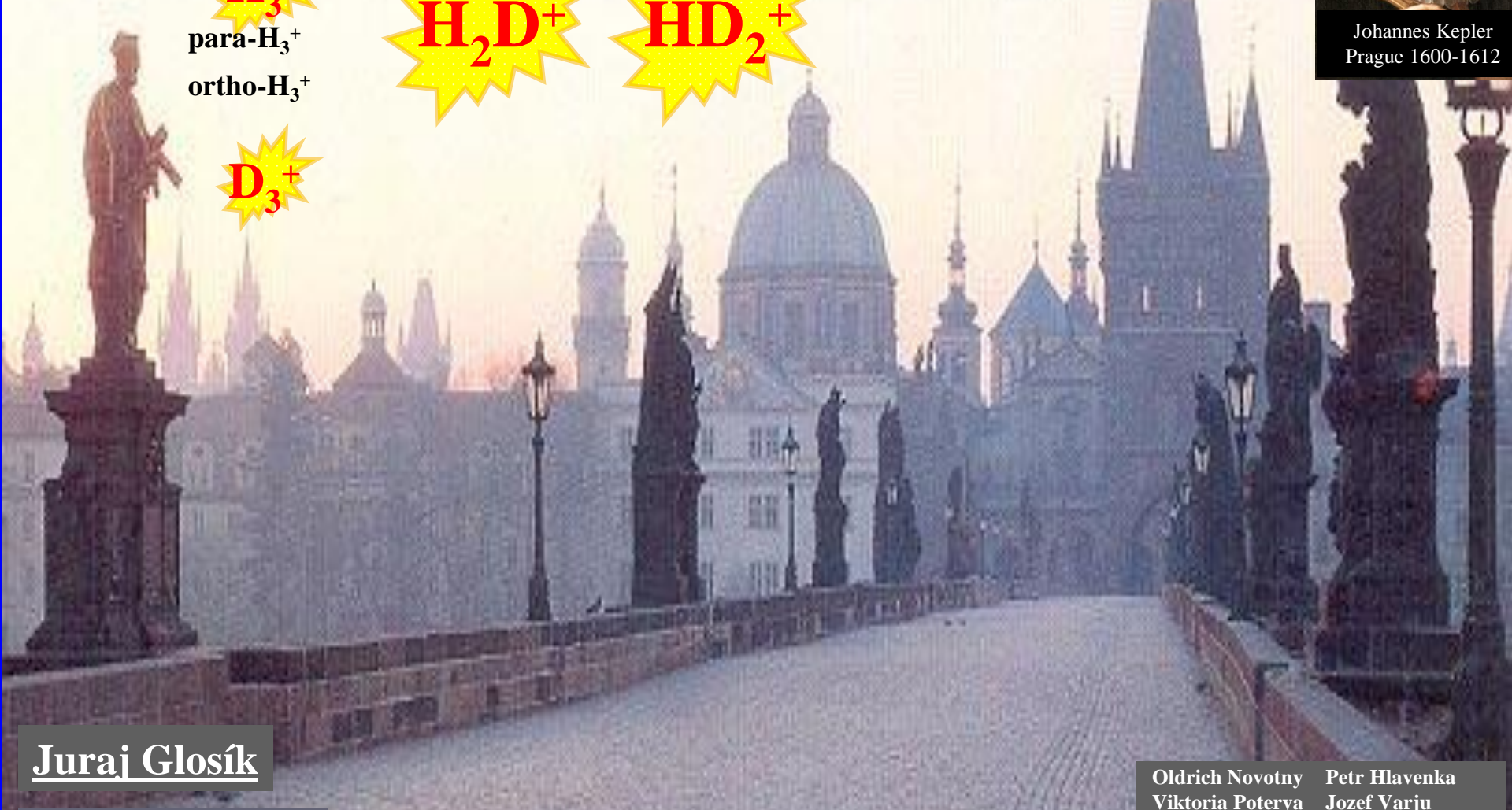
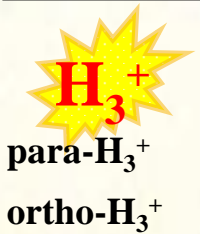
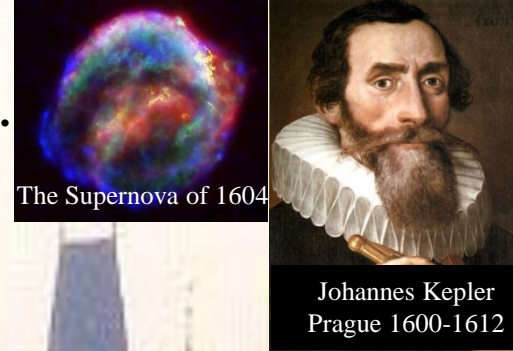
$$k (10 \text{ K}) = \text{????}$$





Laboratory astrophysics

H₂D⁺ and HD₂⁺ recombination with electrons at low temperature.



Juraj Glosík

Charles University

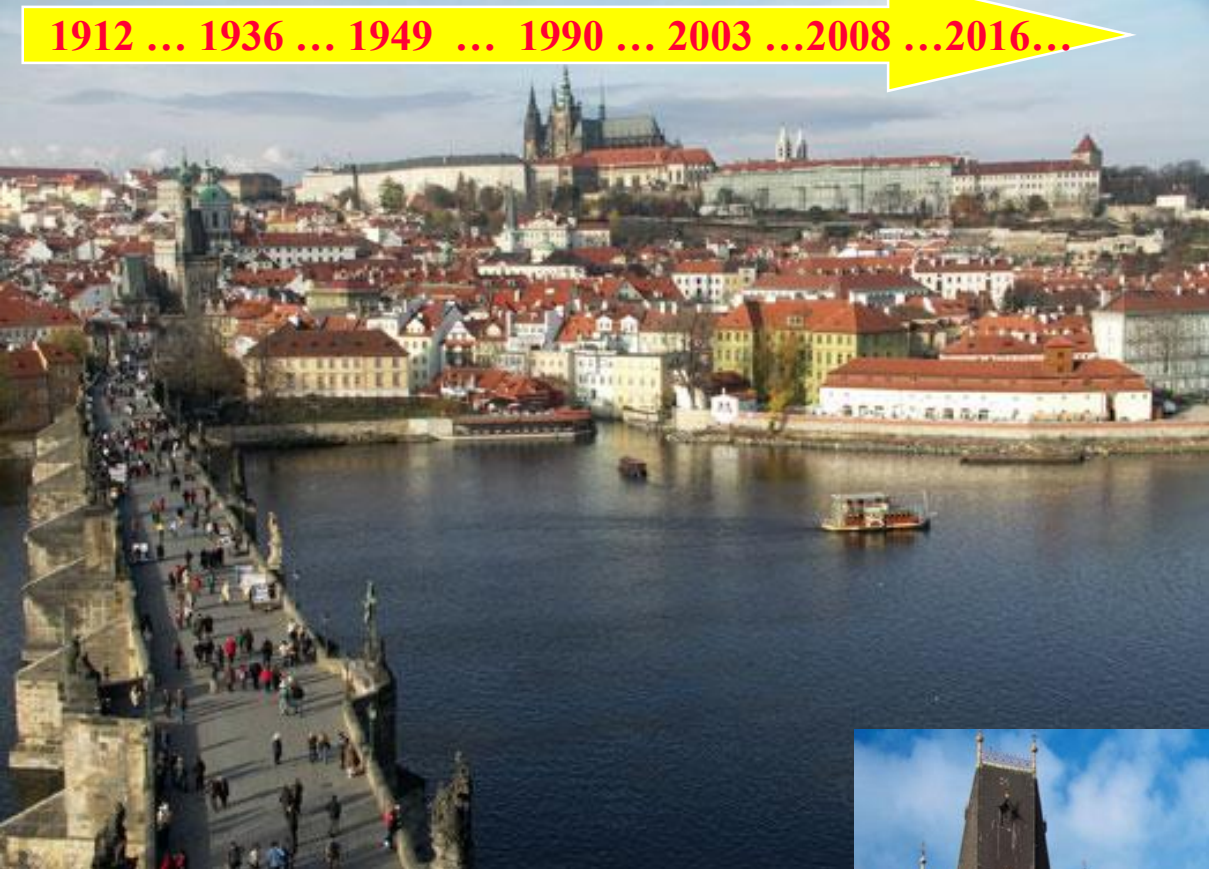
Faculty of Mathematics and Physics

Radek Plašil
Petr Dohnal
Rainer Johnsen

Stepan Roucka
Ábel Kálosi

Oldrich Novotny	Petr Hlavenka
Viktoria Poterya	Jozef Varju
Andryj Pysanenko	Petr Macko
Chris H. Greene	Slava Kokouline
Ihor Korolov	Michal Hejduk
Tomáš Kotrík	Peter Rubovič

1912 ... 1936 ... 1949 ... 1990 ... 2003 ... 2008 ... 2016...



Charles University
Faculty of Mathematics and Physics
Juraj.glosik@mff.cuni.cz



1912 ... 1936 ... 1949 ... 1990 ... 2003 ... 2008 ... 2016 ... 2023

04. 12. 2023



H_3^+ , H_2D^+ , HD_2^+ , D_3^+ are fundamental

A&A 494, 623–636 (2009)
 DOI: 10.1051/0004-6361:200810587
 © ESO 2009

Astronomy
 & Astrophysics

Chemical modeling of L183 (L134N): an estimate of the ortho/para H_2 ratio*

L. Pagani¹, C. Vastel², E. Hugo³, V. Kokouline⁴, C. H. Greene⁵, A. Bacmann⁶,
 E. Bayet⁷, C. Ceccarelli⁶, R. Peng⁸, and S. Schlemmer³

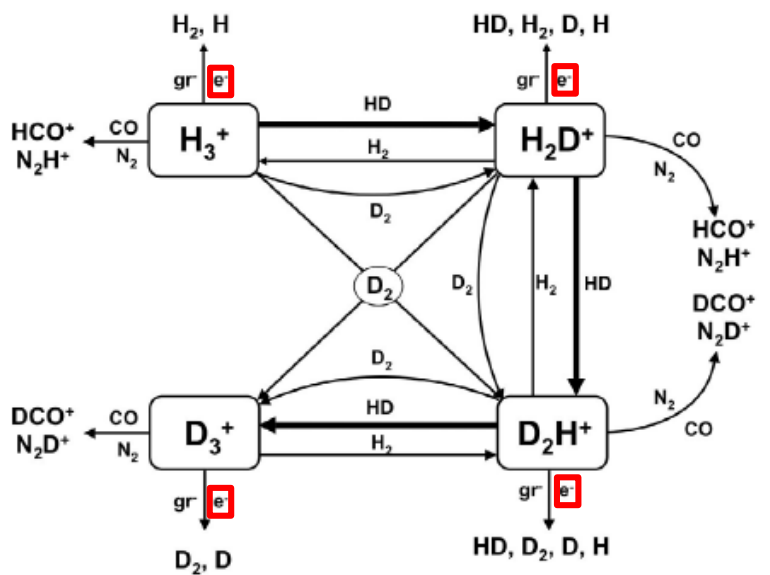
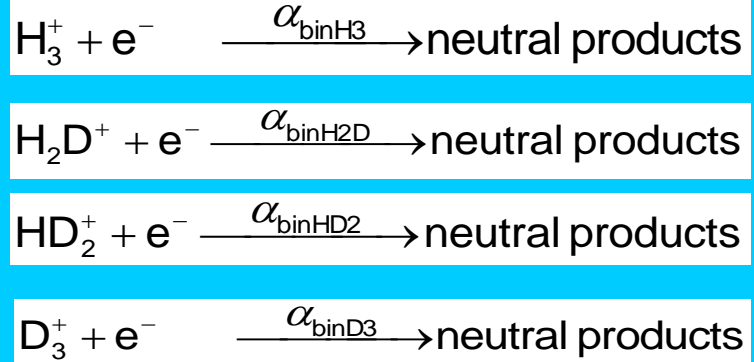


Fig. 4. Main reactions involved in the H_3^+ chemical network. When CO and N_2 are depleted, the reactions with bold arrows are dominant.



H_3^+ , H_2D^+ , HD_2^+ , D_3^+ are fundamental

2009

Chemical modeling of L183 (L134N): an estimate of the ortho/para H_2 ratio*

L. Paganini¹, C. Vastel², E. Hugo³, V. Kokouline⁴, C. H. Greene⁵, A. Bacmann⁶, E. Bayer⁷, C. Ceccarelli⁸, R. Peng⁹, and S. Schlemmer¹⁰

2009

Jahn-Teller Interactions in the Dissociative Recombination of H_3^+

Ch. Jungen^{1,*} and S. T. Pratt²

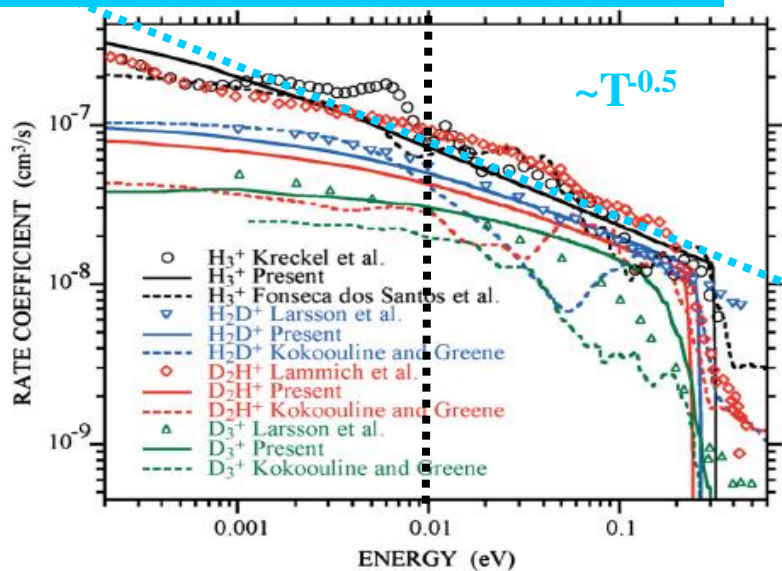
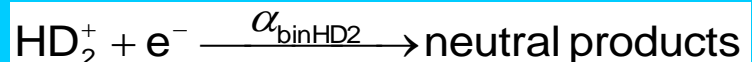
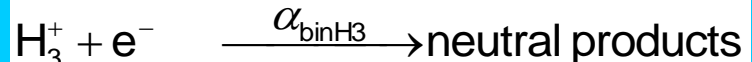
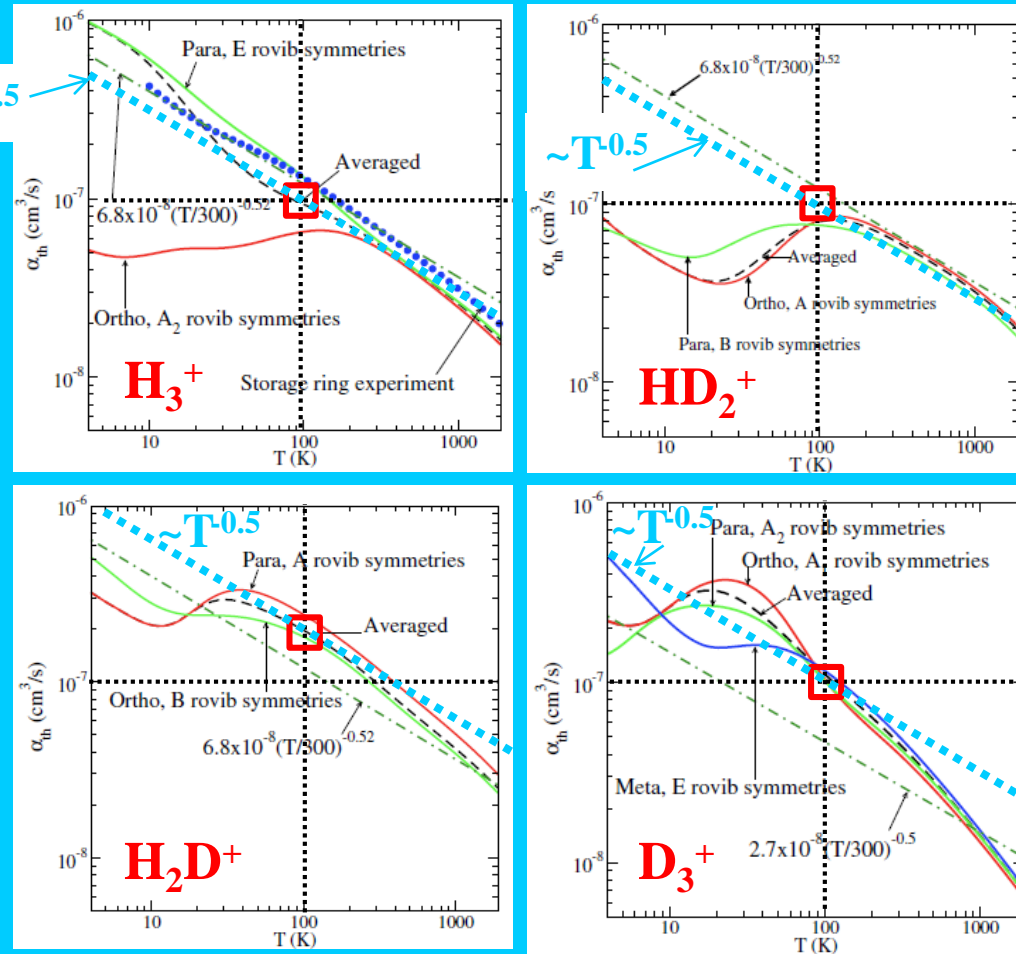


FIG. 3 (color). The DR rate coefficient of an electron and H_3^+ , H_2D^+ , D_2H^+ , and D_3^+ as a function of collision energy. H_3^+

$$\alpha \sim \langle v \cdot \sigma \rangle$$

$$\alpha \sim T^{0.5}$$



B. J. McCall, et al. *Physical Review A* (2004)

H. Kreckel, J. Glosik, et al. *Phys. Rev. Lett.* 2005,

....2008, new improved calculations

L. Pagani¹, C. Vastel², E. Hugo³, V. Kokouline⁴, Chris H. Greene⁵, A. Bacmann⁶, E. Bayet⁷, C. Ceccarelli⁶, R. Peng⁸, and S. Schlemmer³

M. Larsson, B.J. McCall, A.E. Orel (2008)

J. Glosik, R. Plasil, et al. *Phys. Rev. A*, 2009.

H. Kreckel, O. Novotny, et al., *Phys. Rev. A* (2010).

K. N. Crabtree, N. Indriolo, et al., *Astrophys. J.* (2011)

J. Varju, M. Hejduk, J. Glosik, et al. *Phys. Rev. Lett.*, 2011.

P. Dohnal, M. Hejduk, J. Glosik, et al. *J. Chem. Phys.*, 2012.

Doubts 2011

“Presently no rate coefficient measurement with a confirmed temperature below 300 K exists“.

Petrignani *et al.* *Phys. Rev. A* (2011)

Theory of Binary DR

The main mechanism (Jahn-Teller coupling) that leads to the fast dissociation when electron recombines with the ion requires vibrational excitation of ionic core

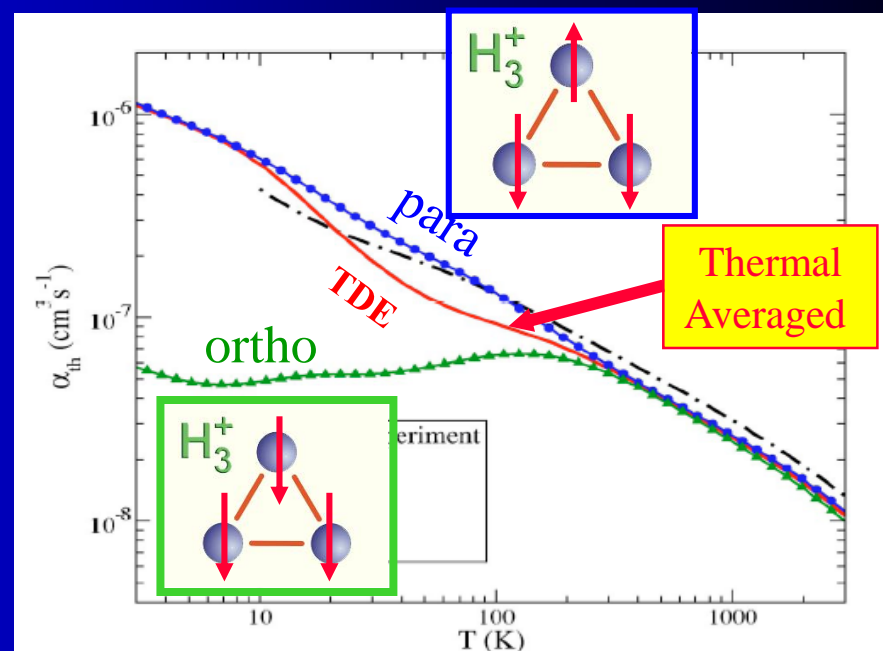


FIG. 5. (Color online) The present theoretical thermal rate coefficient for dissociative recombination of H_3^+ is compared with the experimental rate coefficient deduced from the storage ring experiment of McCall and co-workers (Refs. 9 and 10).

Unfortunately the experiments on storage rings were stopped



3D 60 K

H₃⁺ Potential curves In the case of H₃⁺, a simple 2-dimensional picture of molecular states suggests that recombination should be very inefficient

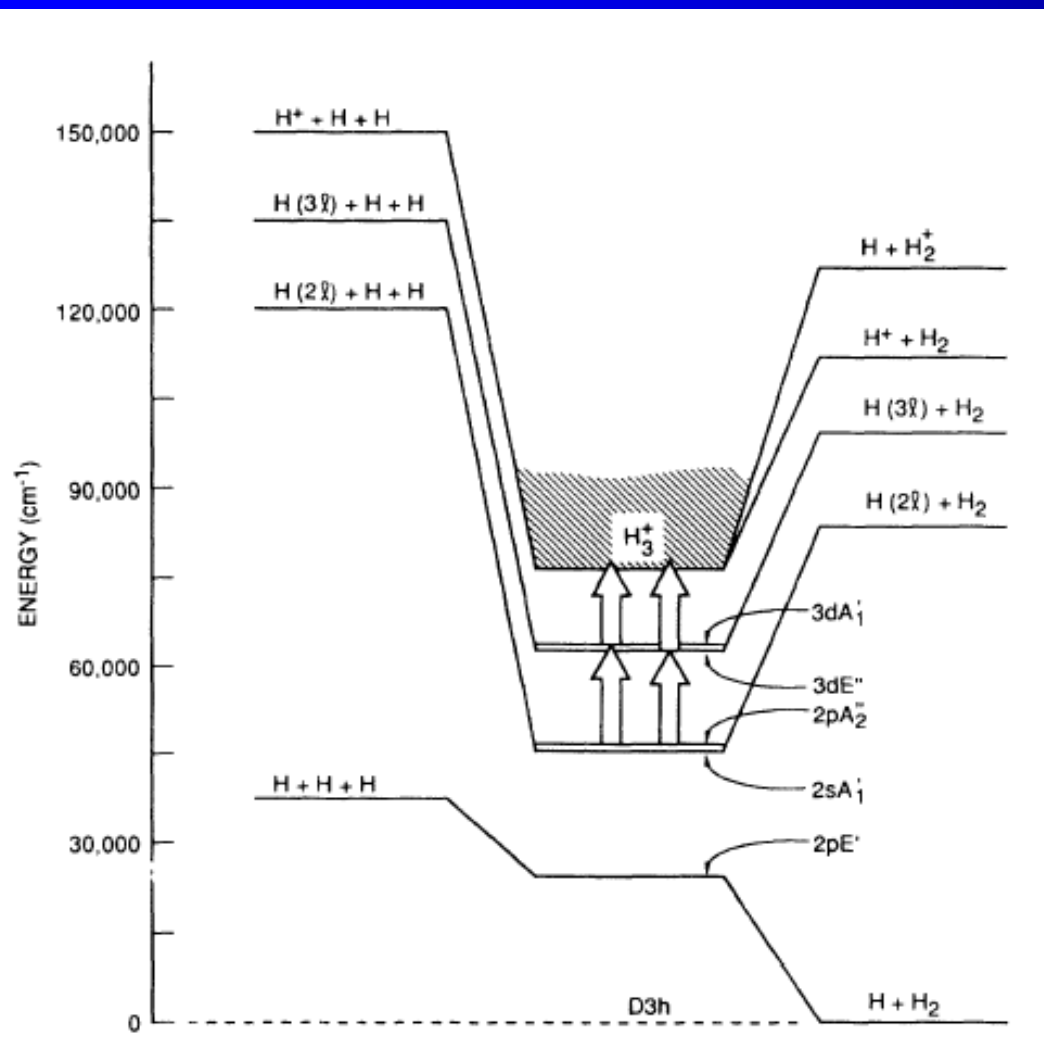
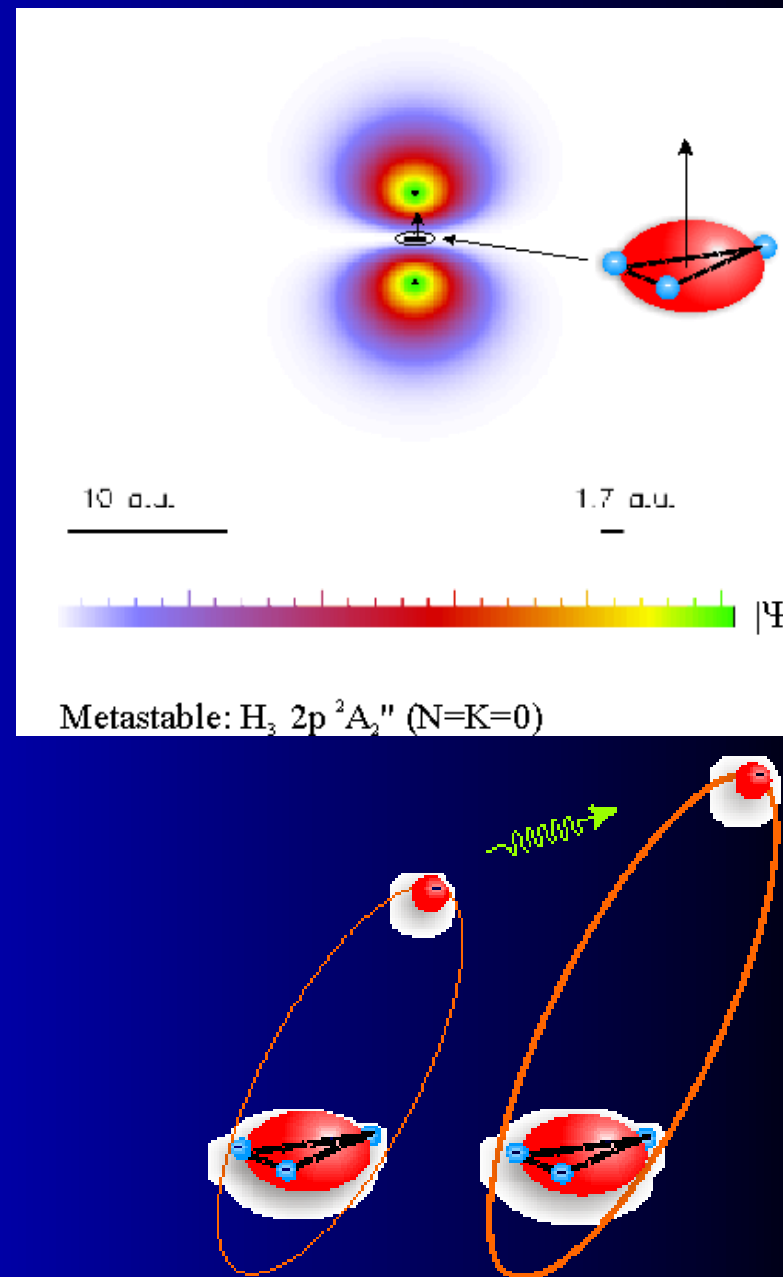
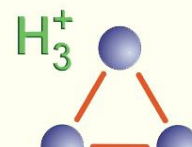


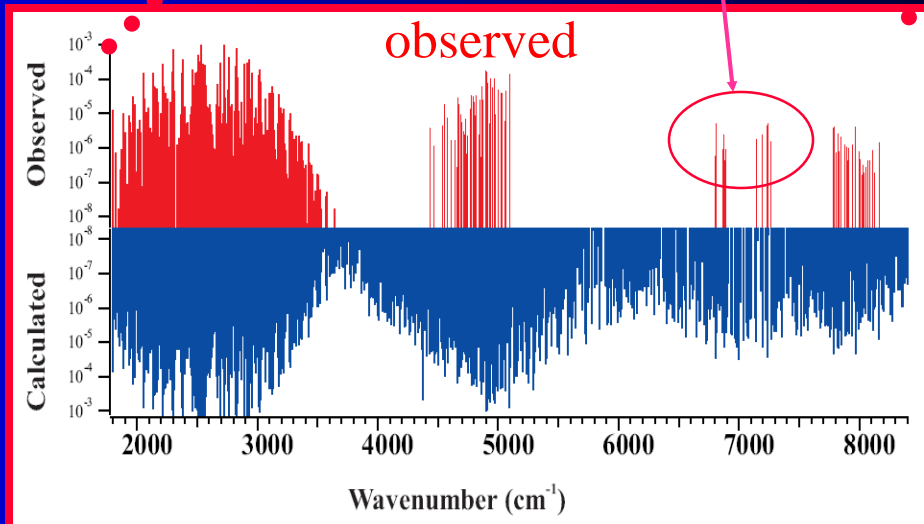
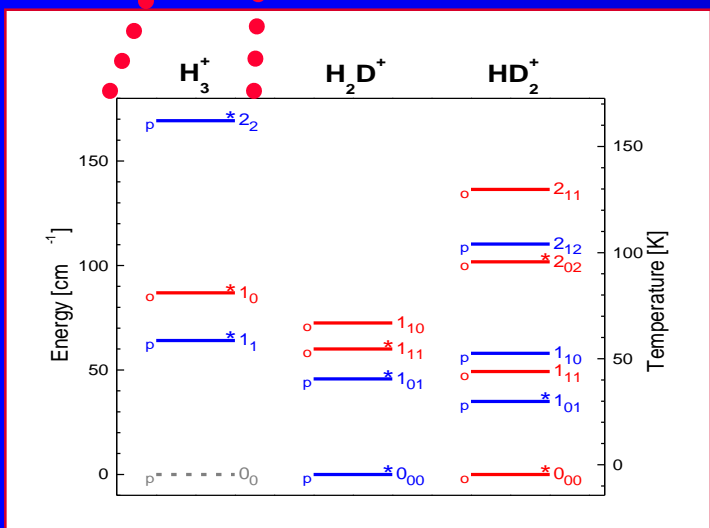
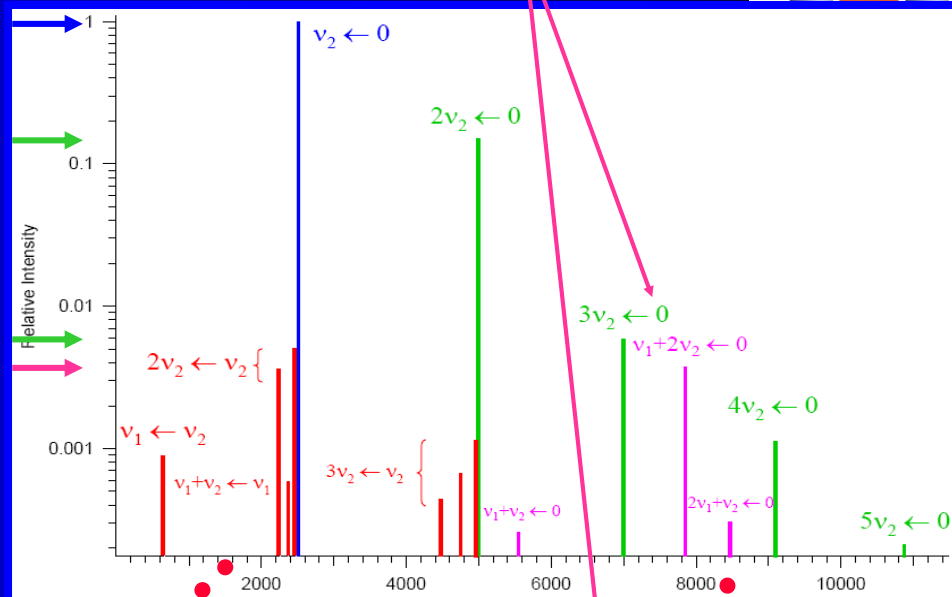
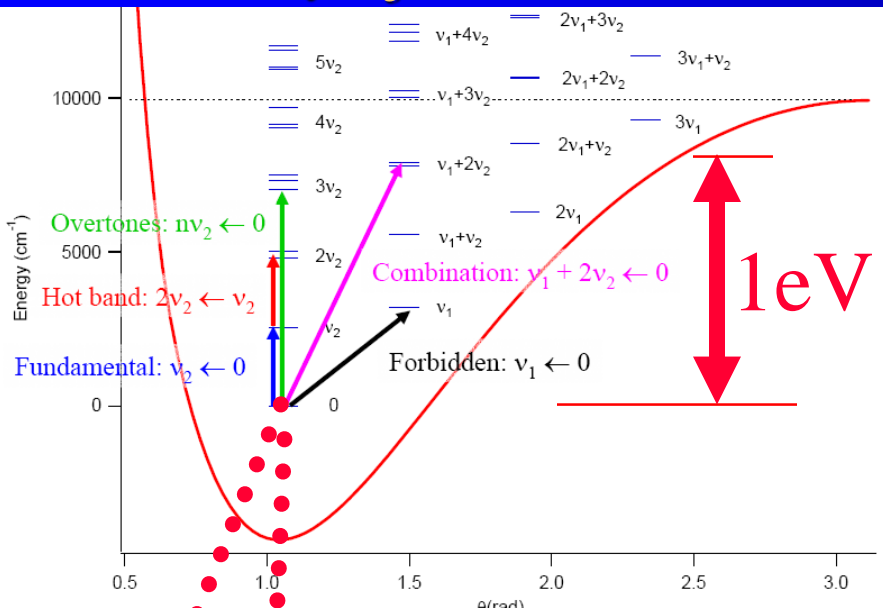
FIG. 1. Energy diagram of triatomic hydrogen (D_{3h} geometry) showing the location of the bound Rydberg states and the unstable ground state of H₃⁺ in relation to the neutral and ionic dissociation limits.



Line intensity H_3^+



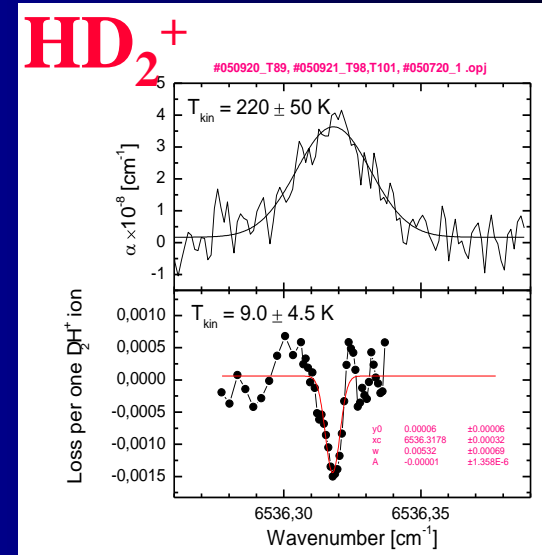
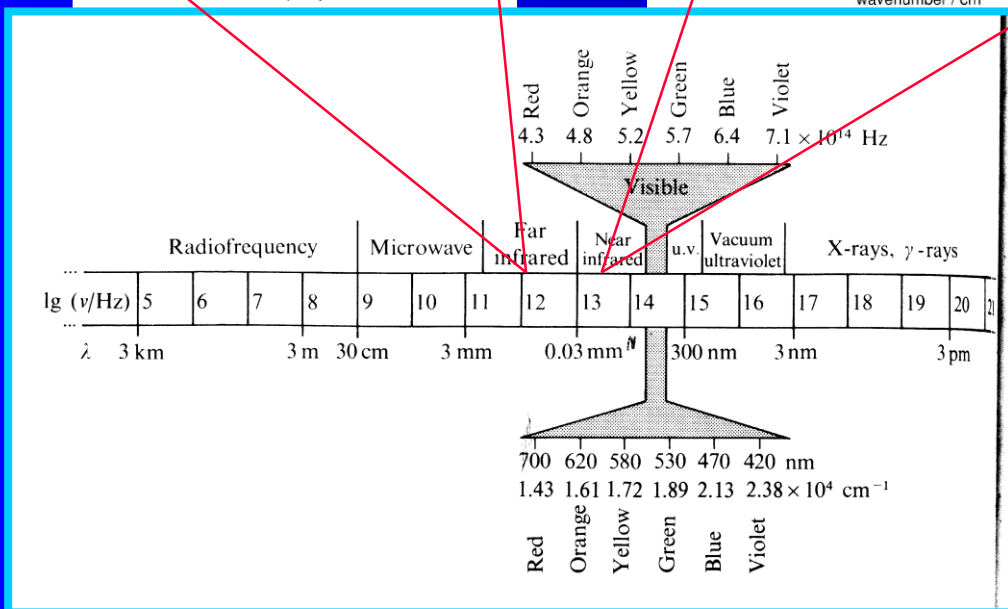
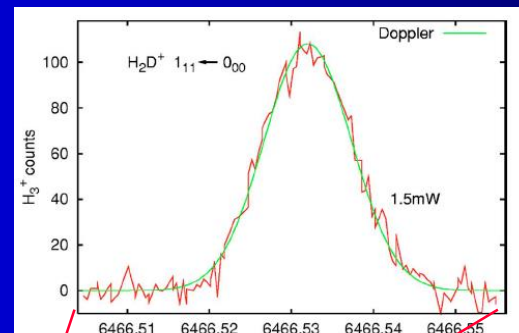
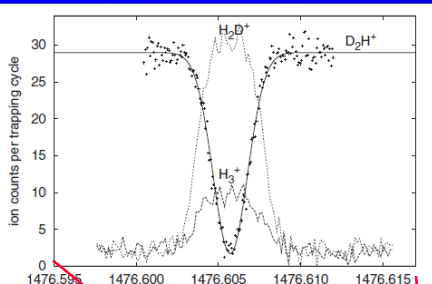
High sensitivity required



LIR - H₂D⁺ and D₂H⁺ precision of 10⁻⁸

precision of $\Delta \nu/\nu = 10^{-8}$.

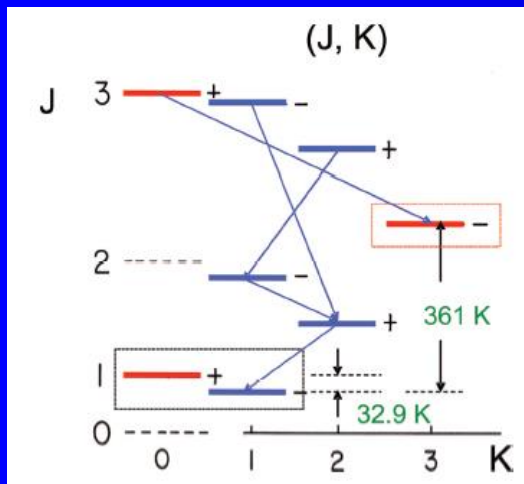
~26K



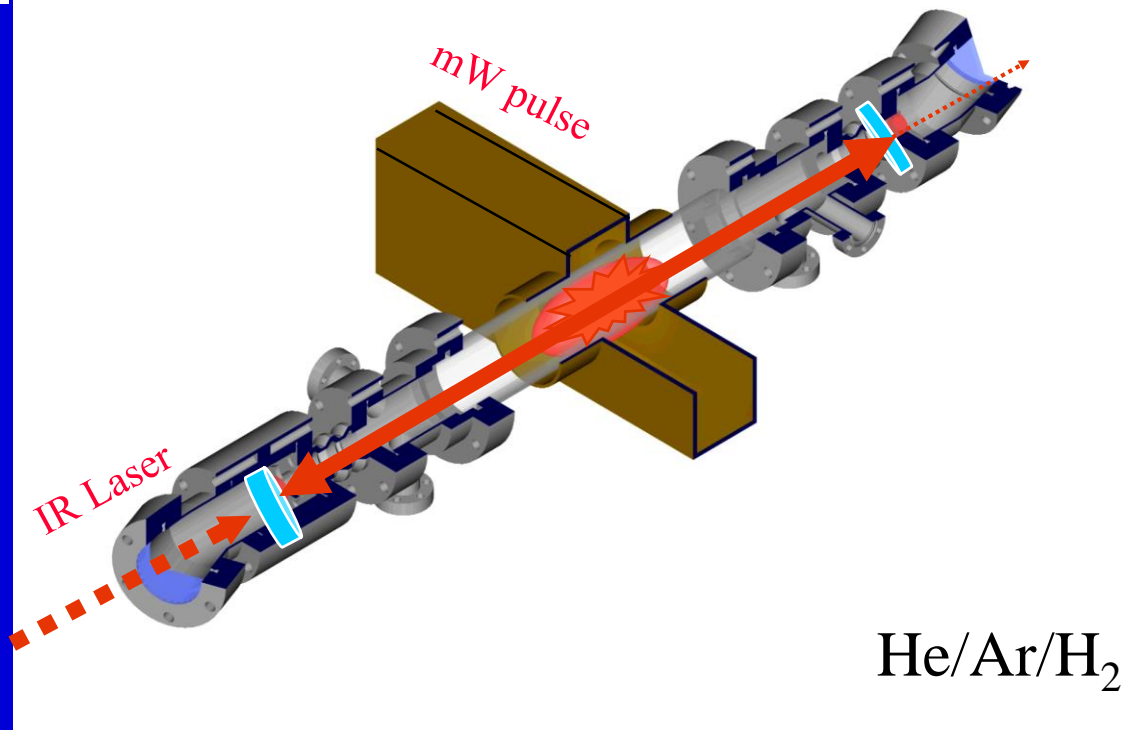
Stationary afterglow + Spectroscopic identification of recombining ions

$$\frac{d[H_3^+]}{dt} = -\alpha[H_3^+]n_e = -\alpha[H_3^+]^2$$

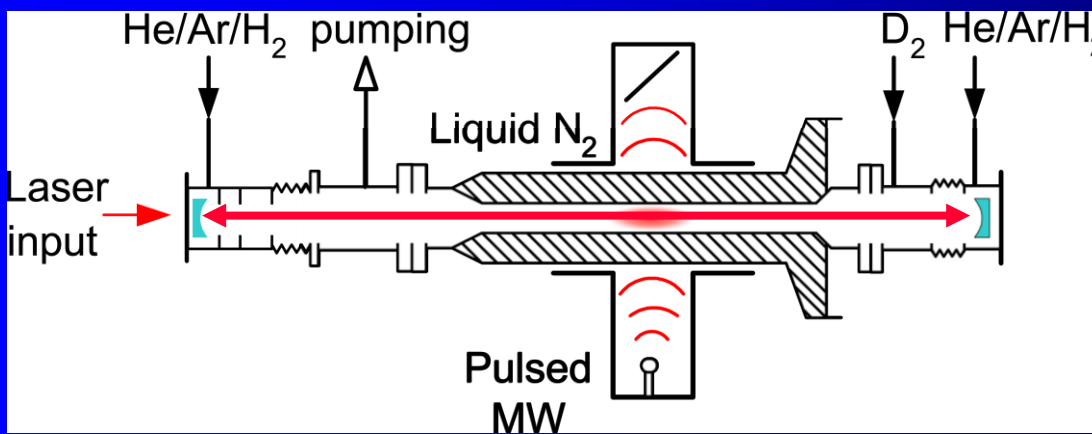
IR-CRDS
Laser absorption spectroscopy



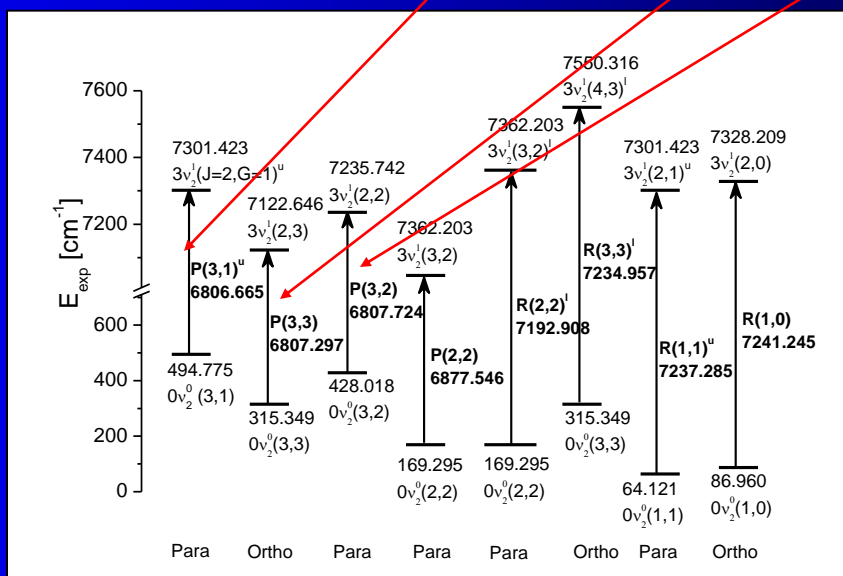
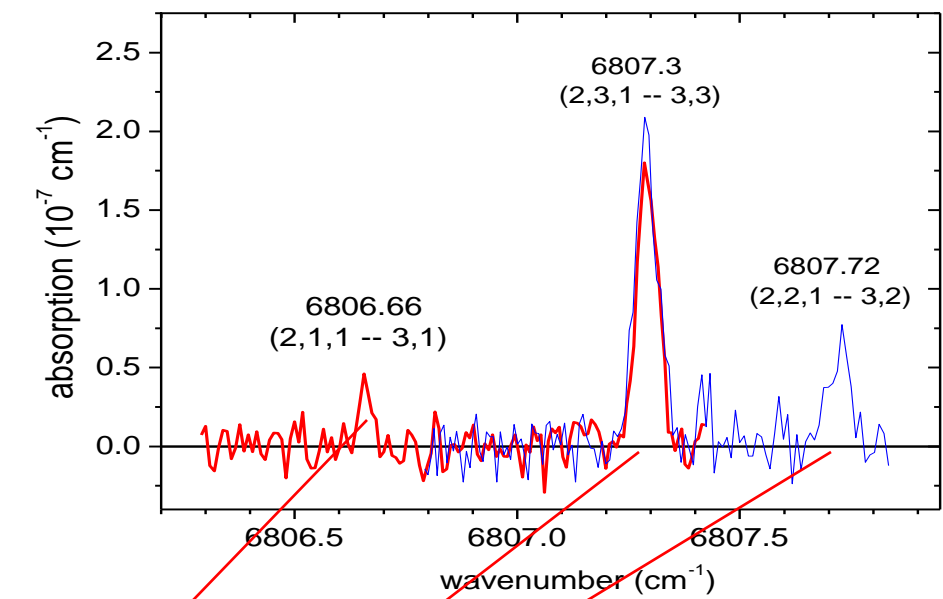
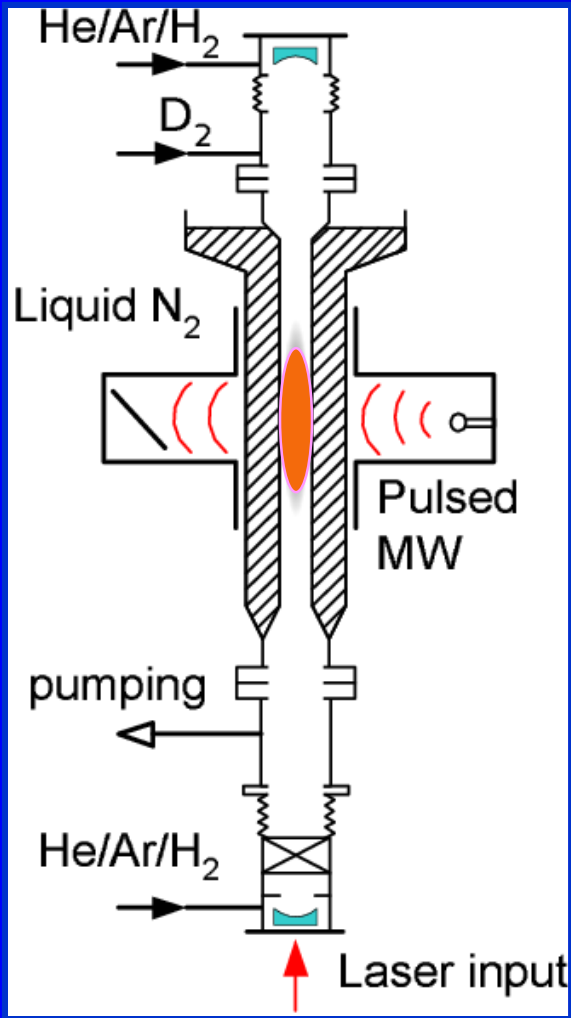
CRDS



He/Ar/H₂



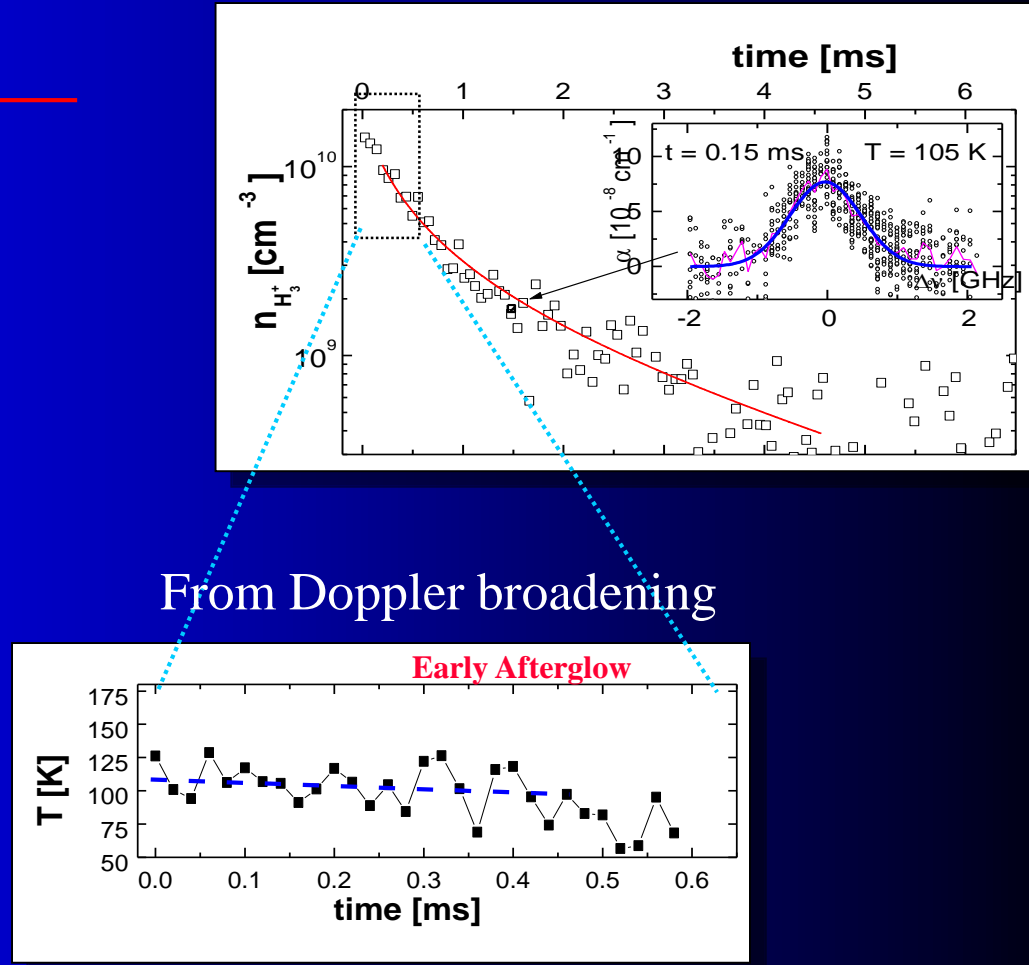
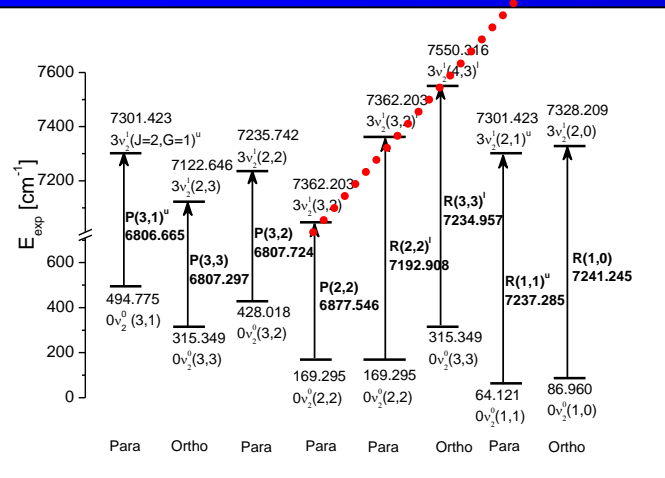
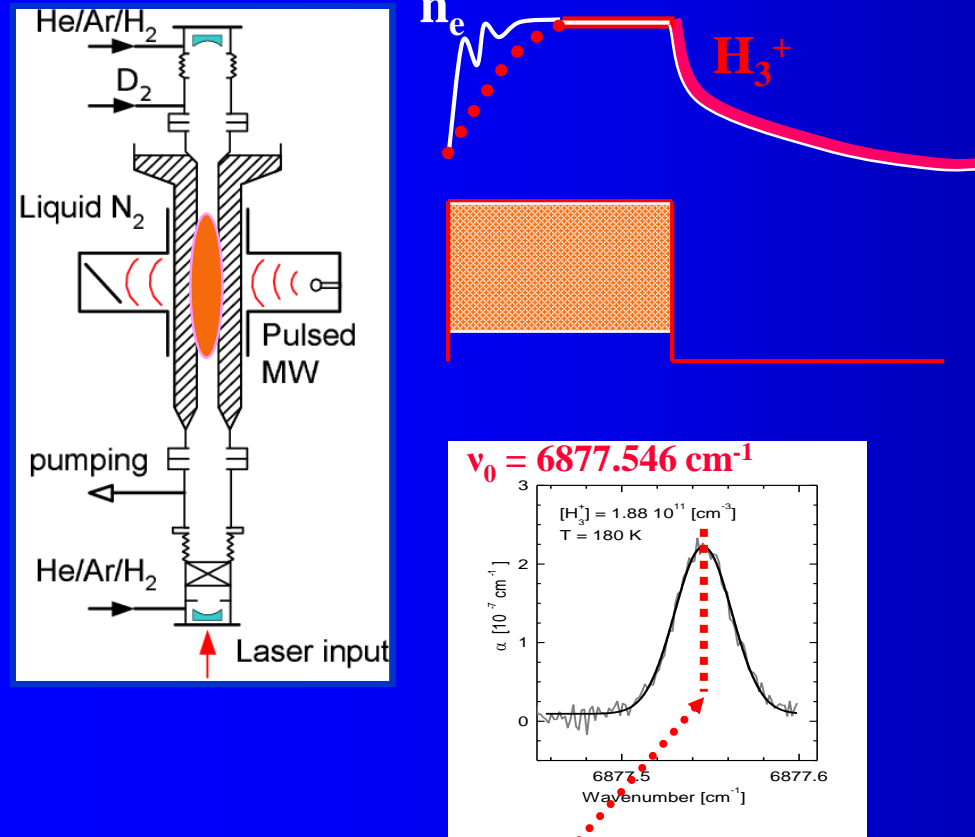
Spectrum - He/Ar/H₂ microwave discharge



1469nm

1381nm

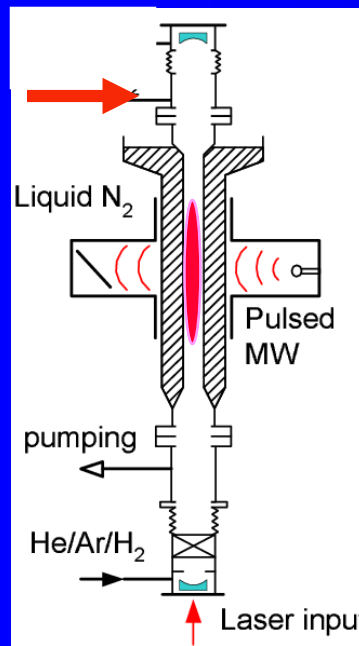
Pulsed discharge – plasma decay



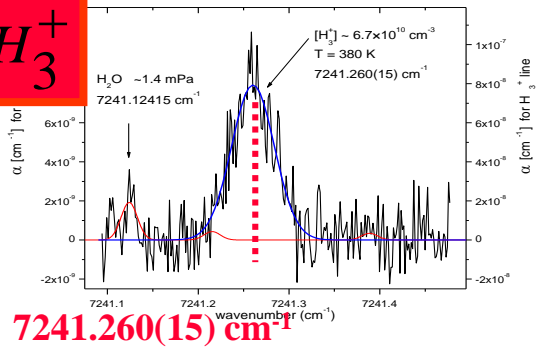
From Doppler broadening

Absorption studies

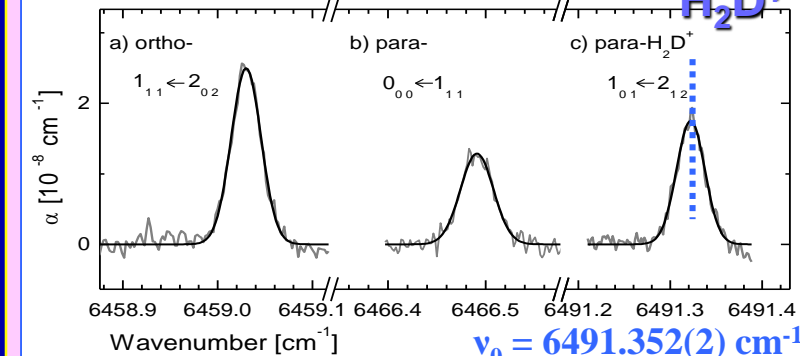
He/Ar/H₂/D₂



H₃⁺

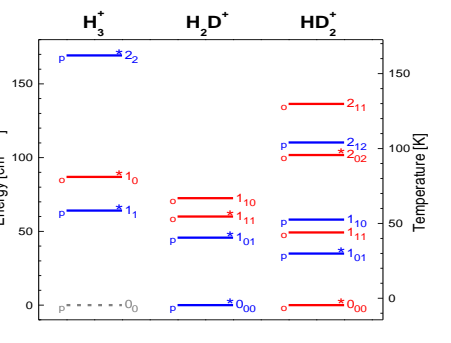
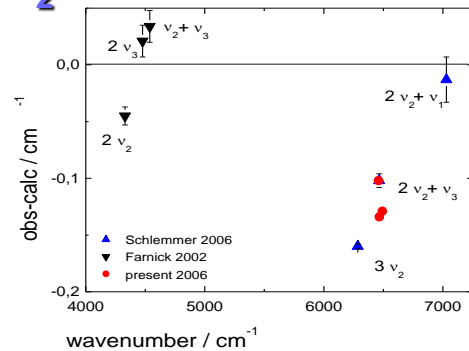


H₂D⁺ (2v₂ + v₃ ← 0)

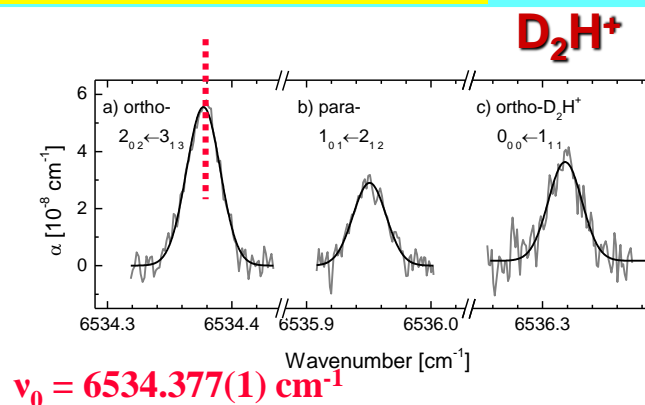


Combination band

H₂D⁺



D₂H⁺ (v₁ + 2v₃ ← 0)



Combination band

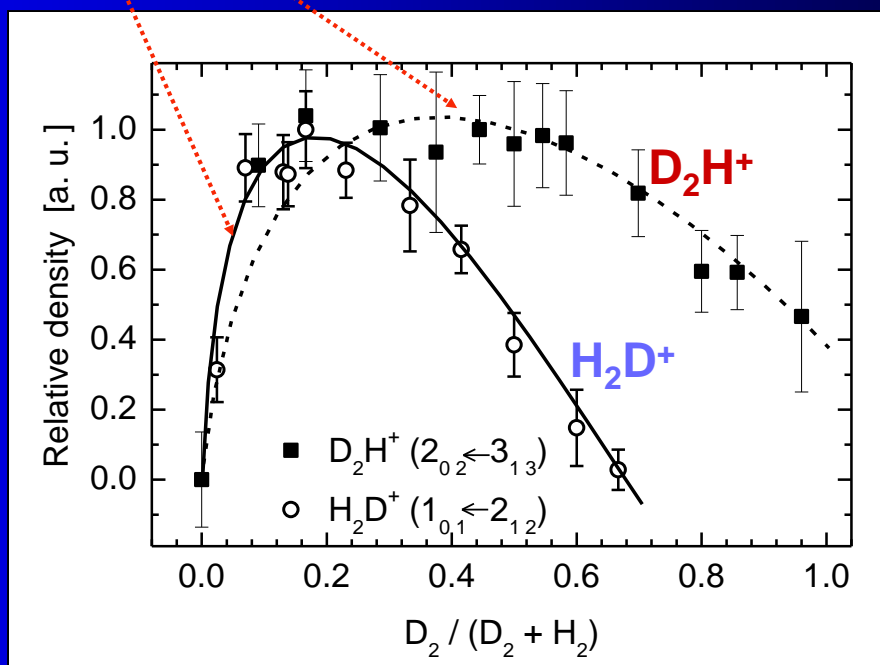
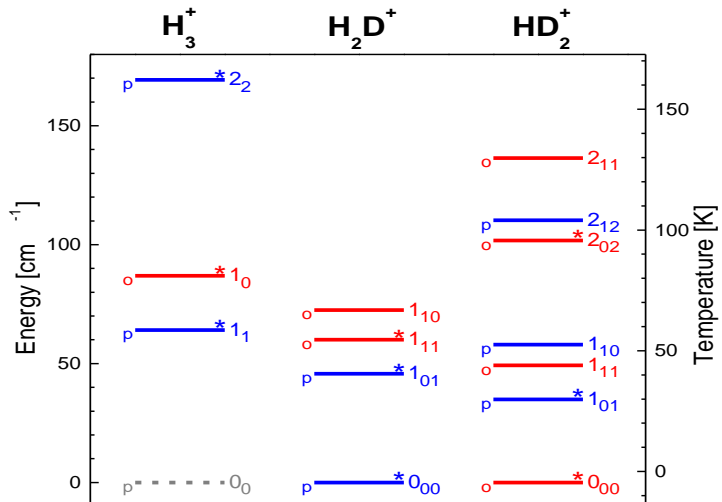
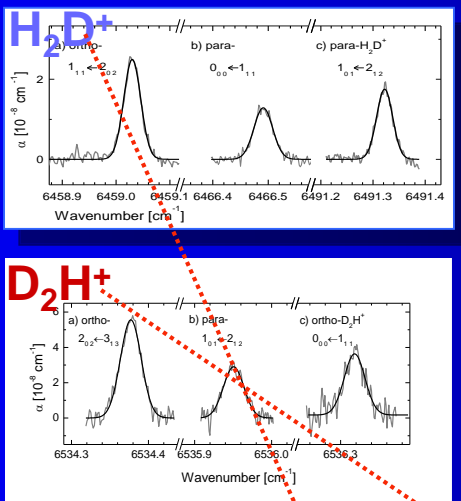
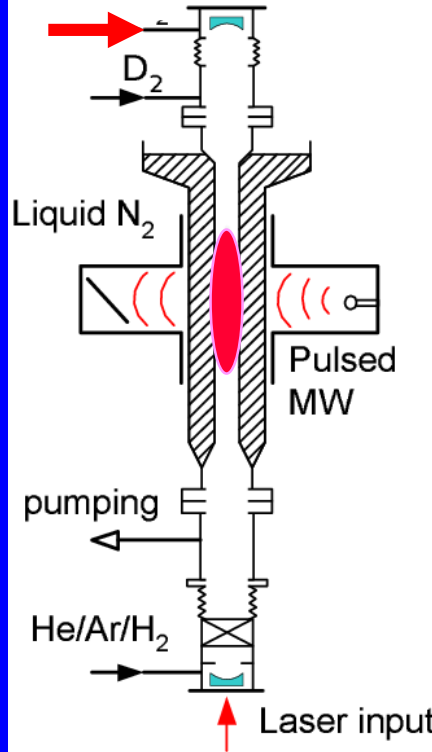
E'[K]	Wavenumber [cm ⁻¹]		$\nu_{\text{Theor}} - \nu_{\text{Exp}}$
	ν_{Exp}	ν_{Theor}	
146.3	6534.377(1)	6534.374	0.003
50.2	6535.950(1)	6535.943	0.007
0	6536.319(2)	6536.301	0.018

D₃⁺

???

Ionic composition of H₂/D₂ plasma

He/Ar/H₂/D₂

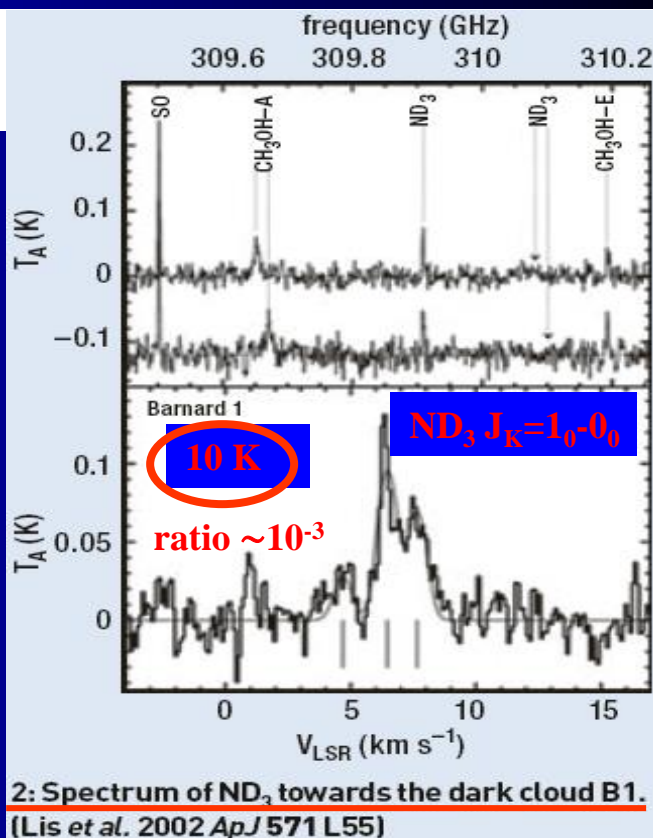
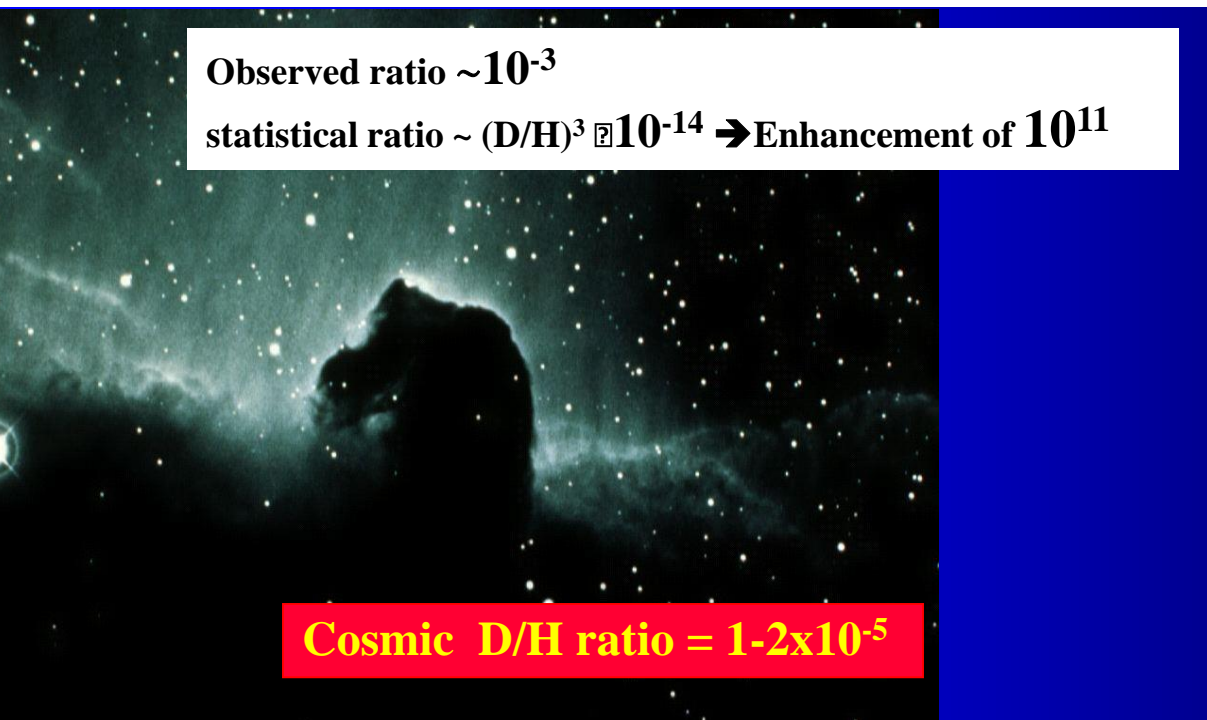


Observation of high population of deuterated molecules

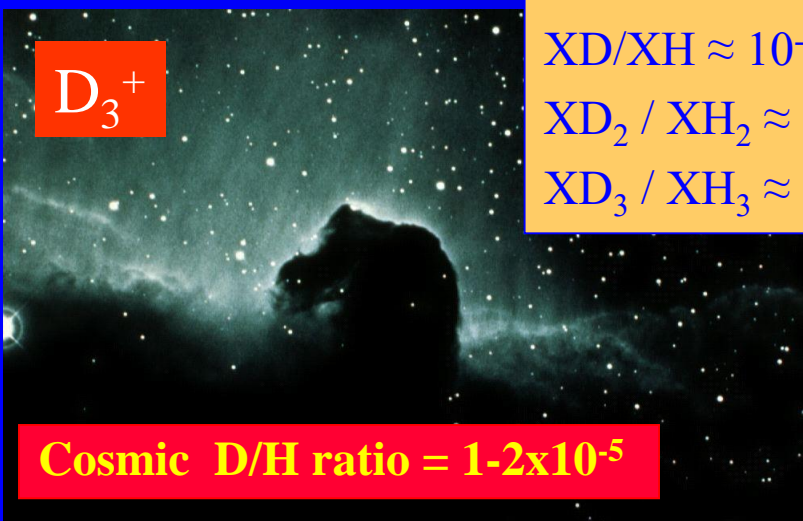
The first detection of deuterated molecules were made in the early 1970s..... Observed enhancement of D in molecules

H_2D^+	Stark	(1999)	$1_{10}-1_{11}$ transition of ortho- emission from young stellar object NGC 1333 IRAS4A.
H_2D^+	Caselli	(2003)	detected towards L1544.
HD_2^+	Vastel	(2004)	the first detection
$\text{CH}_2\text{DOH}...$	Parise	(2003, 2004)	have detected 4 isotopomers of deuterated methanol
NHD_2/NH_3	Roueff	(2000)	
	Loinard	(2001)	is 0.005 in the cold cloud L134N and 0.03 in the low-mass protostar 16293 E
$\text{D}_2\text{CO}/\text{H}_2\text{CO}$	Loinard	(2002)	
	Bacmann	(2003)	is between 0.01 and 0.4 in a low-mass protostars and prestellar cores
$\text{NH}_2\text{D}/\text{NH}_3$	J. Hatchell	(2003)	high ratios~4–33% in protostellar cores
ND_3/NH_3	Lis	(2002)	ratio $\sim 10^{-3}$ cold dense Barnard 1 cloud
	Tak	(2002)	Class 0 protostar NGC 1333 IRAS4A

Observed ratio $\sim 10^{-3}$
statistical ratio $\sim (\text{D/H})^3 \approx 10^{-14} \rightarrow$ Enhancement of 10^{11}



High population of deuterated molecules



$Cosmic\ D/H \approx 10^{-5}$
 $XD/XH \approx 10^{-1}-10^{-3}$
 $XD_2 / XH_2 \approx 10^{-2}$
 $XD_3 / XH_3 \approx 10^{-3}$

	H_3^+	H_2D^+	D_2H^+	D_3^+
HD				
N_2D^+		DCO^+		DCN
DNC		$HDCS$		D_2CS
HDO		DC_3N		DC_5N
C_3HD		$HDCO$		D_2CO
CH_3OD		CH_2DOH		CHD_2OH
CD_3OH		CH_2DCN		NH_2D
NHD_2		ND_3		CHD_2CCH
CH_3CCD		C_2D		C_4D
HDS		D_2S		

Deuterated molecules that have been detected in interstellar clouds as of February 2005.

Species	Observed ratio
NH_2D/NH_3	0.01
$HDCO/H_2CO$	0.005-0.11
DCN/HCN	0.023
DNC/HNC	0.015
C_2D/C_2H	0.01
DCO^+/HCO^+	0.02
N_2D^+/N_2H^+	0.08
DC_3N/HC_3N	0.03-0.1
$HDCS/H_2CS$	0.02

Gas phase reactions,

ion-molecule reactions,
recombination

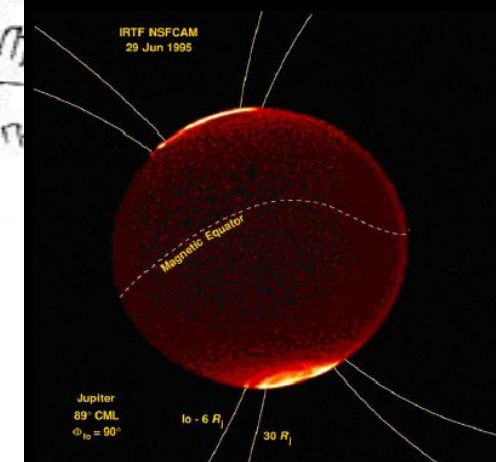
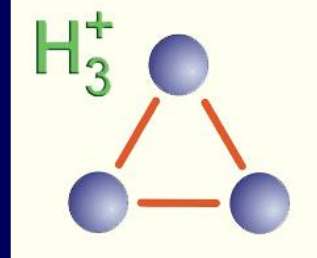
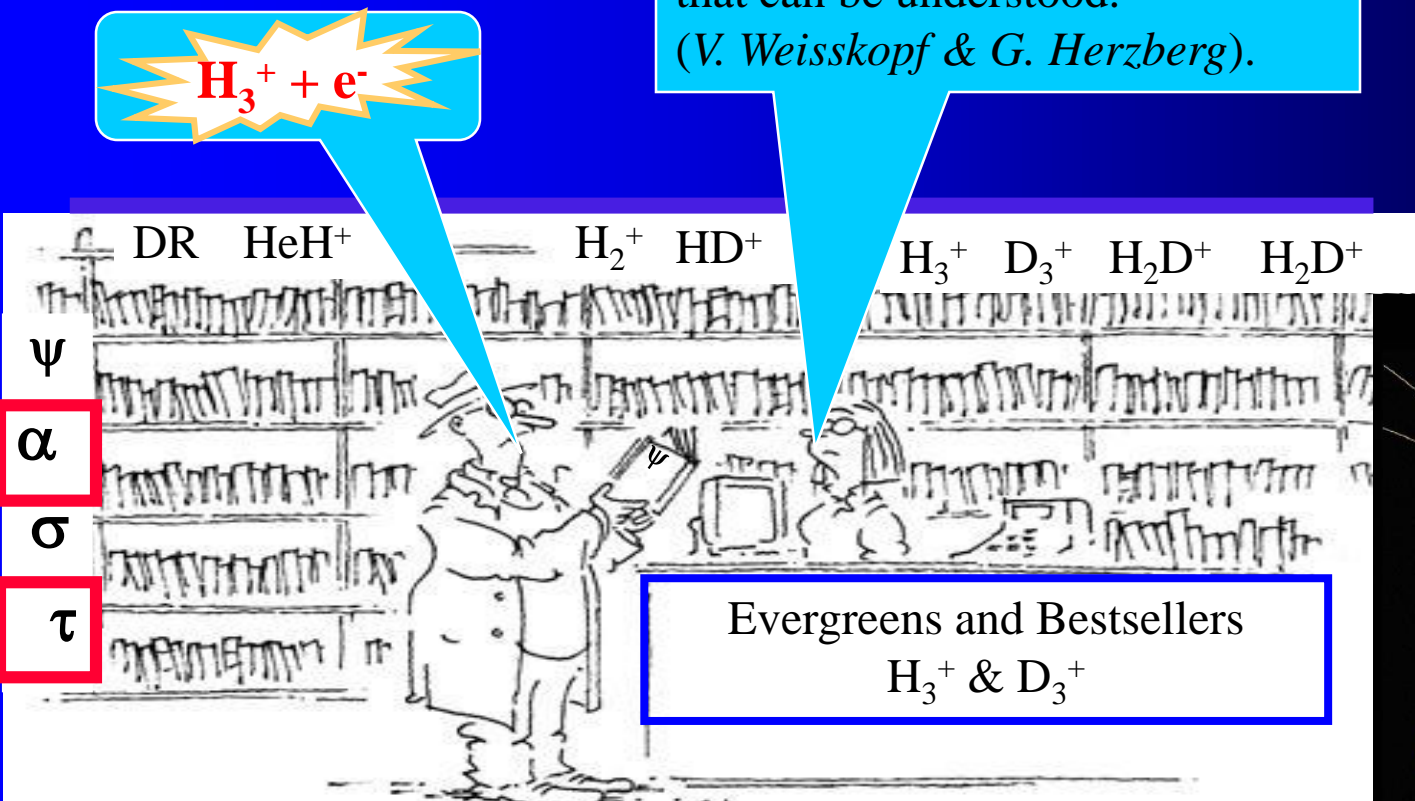
Grain surface reactions

Physics of condensation and evaporation from grain surface

Different views
& different plasmas

H_3^+ and its interaction of with e^- is FUNDAMENTAL

If you understand hydrogen,
you understand all
that can be understood.
(V. Weisskopf & G. Herzberg).



H_3^+ , H_2D^+ , HD_2^+ , D_3^+ are fundamental

A&A 494, 623-636 (2009)
DOI: 10.1051/0004-6361:200810587
© ESO 2009

Astronomy & Astrophysics

Chemical modeling of L183 (L134N): an estimate of the ortho/para H_2 ratio*

L. Paganini¹, C. Vastel², E. Hugo³, V. Kokouline⁴, C.-H. Greene⁵, A. Bacmann⁶, E. Bayet⁷, C. Ceccarelli⁸, R. Ponç⁹, and S. Schlemmer¹

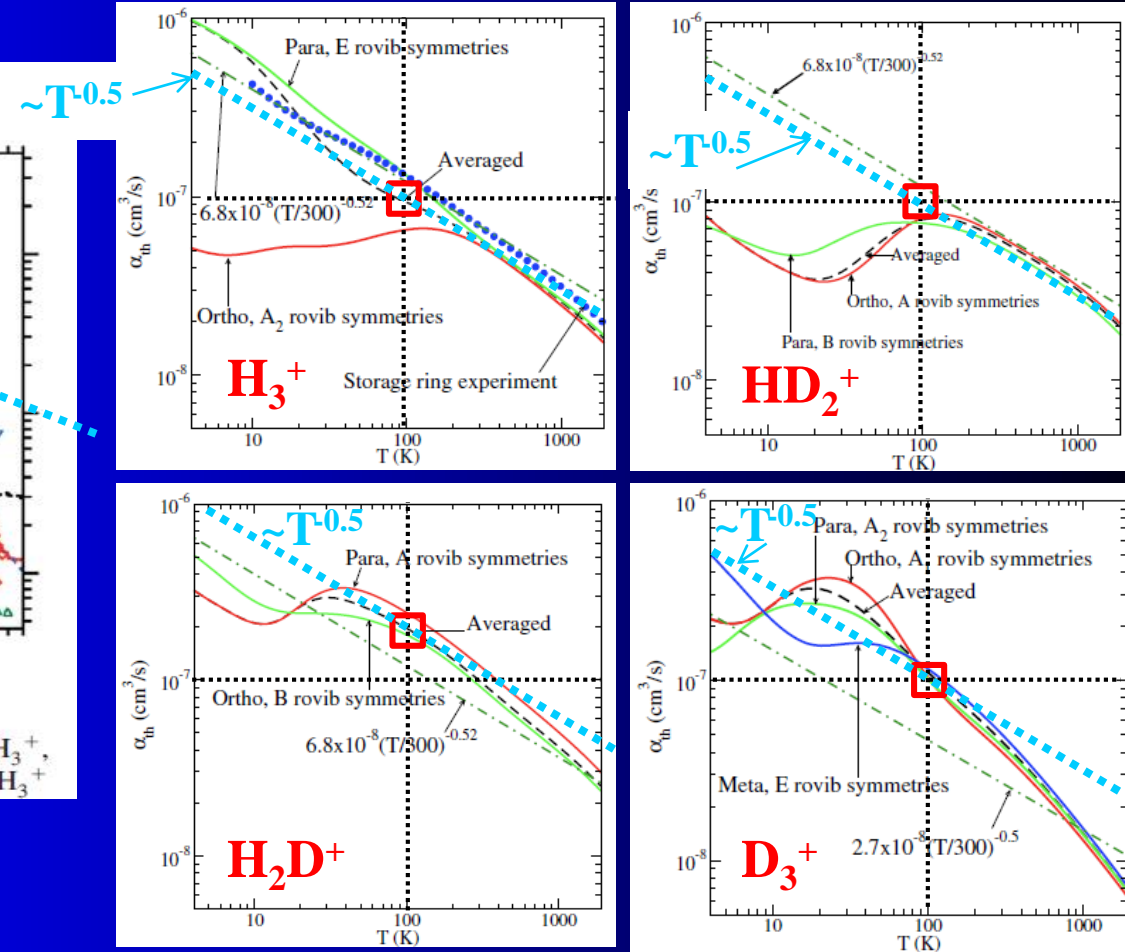
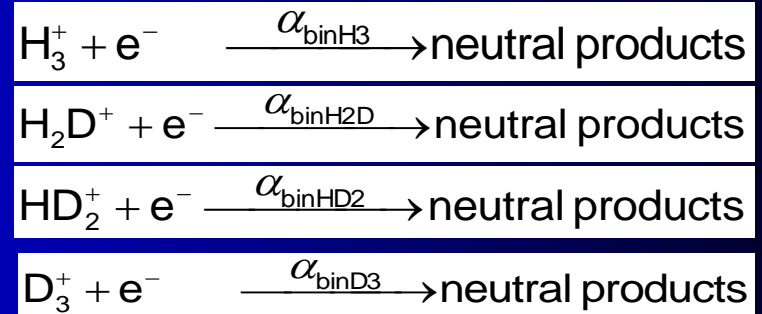


FIG. 3 (color). The DR rate coefficient of an electron and H_3^+ , H_2D^+ , D_2H^+ , and D_3^+ as a function of collision energy. H_3^+

$$\alpha \sim \langle v \cdot \sigma \rangle$$

$$\alpha \sim T^{0.5}$$



H_3^+ interaction with e^-

Plasma Sources Sci. Technol. 24 (2015) 065017

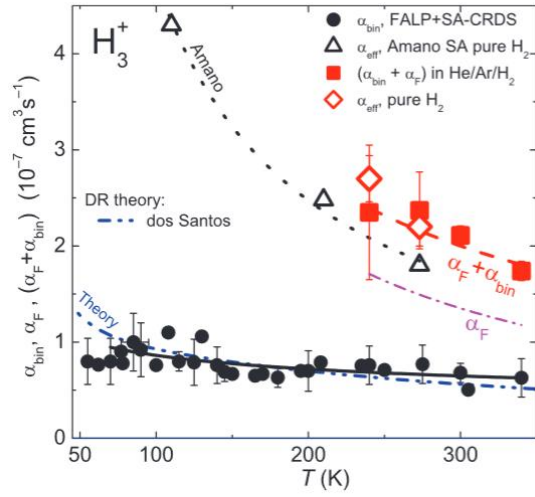


Figure 5. Temperature dependences of α_{bin} , α_F , and their sum ($\alpha_{\text{bin}} + \alpha_F$). The diamonds and squares indicate ($\alpha_{\text{bin}} + \alpha_F$) measured in pure H_2 and in $\text{He}/\text{Ar}/\text{H}_2$ mixture, respectively. The fit of the data (dashed line) gives the temperature dependence: $(\alpha_{\text{bin}} + \alpha_F) = (2.0 \pm 0.4) \times 10^{-7} (T/300 \text{ K})^{-(0.81 \pm 0.30)} \text{ cm}^3 \text{ s}^{-1}$. The filled circles indicate the values of α_{bin} for H_3^+ ions in $\text{He}/\text{Ar}/\text{H}_2$ mixtures that were obtained in several stationary and flowing afterglow experiments (for details see [22, 26]). The full line indicates the dependence $\alpha_{\text{bin}} = (6.5 \pm 1.4) \times 10^{-8} (T/300 \text{ K})^{-(0.26 \pm 0.07)} \text{ cm}^3 \text{ s}^{-1}$ obtained by fitting α_{bin} data at temperatures 80–340 K. Included are the present data and data from [22, 26]. The dependence of α_F on temperature (dot-dashed line) was obtained by subtracting α_{bin} (full line) from the sum of ($\alpha_{\text{bin}} + \alpha_F$) (dashed line). The rate coefficients measured by Amano [30] in pure H_2 , assumed to be due to binary recombination only, are plotted as open triangles for comparison. The dotted line indicates a fit to Amano's data: $\alpha_{\text{Amano}} = 1.7 \times 10^{-7} (T/300 \text{ K})^{-0.94} \text{ cm}^3 \text{ s}^{-1}$. The theoretical temperature dependence of the binary rate coefficient of dissociative recombination of H_3^+ ions calculated by Fonseca dos Santos *et al.* [12] is plotted by a double dot-dashed line denoted Theory.

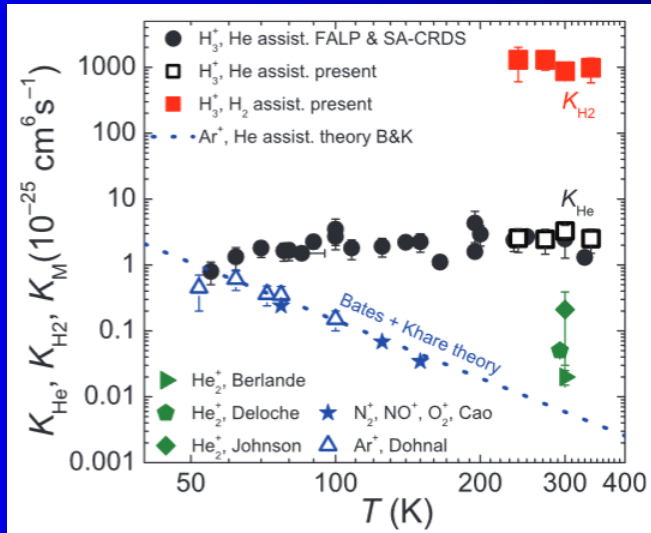


Figure 6. Temperature dependences of the three-body rate coefficients $K_{\text{H}2}$ (closed squares) and K_{He} (open squares) of H_2 and He assisted recombination of H_3^+ ions. Closed circles: K_{He} of H_3^+ ions obtained in our previous experiments [21, 23, 24, 34]. Open triangles: Three-body recombination rate coefficients of He-assisted collisional radiative recombination K_{HeAr^+} of Ar^+ ions measured in a Cryo-FALP II experiment [50]. Filled stars: $K_{\text{He-CRR}}$ as measured by Cao *et al.* [51] for a mixture of atmospheric ions in He. Dotted line: Theoretical dependence of Bates and Khare [32] scaled for Ar^+ ions in He by the reduced mass. Full triangle, pentagon and diamond indicate three-body rate coefficients measured for He_2^+ ions in helium by Berlande [52], Deloche [53] and Johnson [54], respectively.

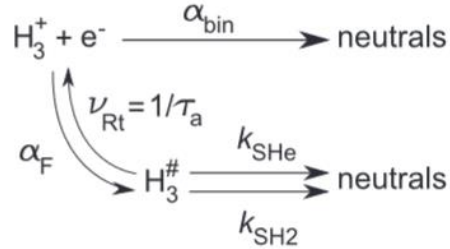


FIG. 1. The scheme of the proposed H_3^+ recombination mechanism. Used symbols are explained in the text.

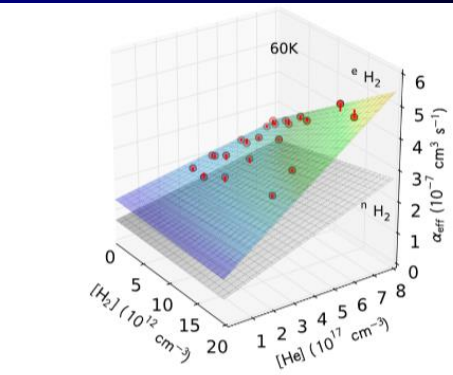


FIG. 7. Cryo-FALP II data. Dependence of ${}^3\alpha_{\text{eff}}$ and ${}^4\alpha_{\text{eff}}$ on [He] and $n_{\text{H}2}$ measured at $T = 60 \text{ K}$ in experiments with ${}^3\text{H}_2$ and with ${}^4\text{H}_2$, respectively. The upper surface is a fit of Eq. (6) to the data (indicated by circles) obtained with ${}^3\text{H}_2$. The lower surface represents a fit of Eq. (6) to the data obtained with ${}^4\text{H}_2$ (data points are omitted for clarity). The data points deviate from the surfaces by amounts on the order $< 2 \times 10^{-8} \text{ cm}^3 \text{ s}^{-1}$ as is shown by red lines connecting the data points with the plane. The parameters of the fits are listed in Table I.

H_3^+ interaction with e^-

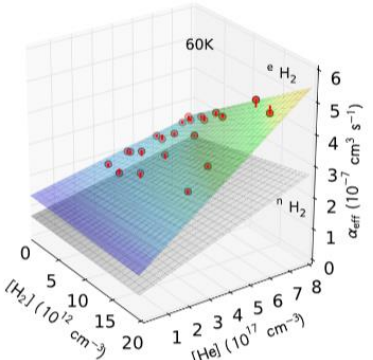


FIG. 7. Cryo-FALP II data. Dependence of ${}^e\alpha_{\text{eff}}$ and ${}^n\alpha_{\text{eff}}$ on $[\text{He}]$ and $[\text{H}_2]$ measured at $T = 60 \text{ K}$ in experiments with ${}^e\text{H}_2$ and with ${}^n\text{H}_2$, respectively. The upper surface is a fit of Eq. (6) to the data (indicated by circles) obtained with ${}^e\text{H}_2$. The lower surface represents a fit of Eq. (6) to the data obtained with ${}^n\text{H}_2$ (data points are omitted for clarity). The data points deviate from the surfaces by amounts on the order $<2 \times 10^{-8} \text{ cm}^3 \text{ s}^{-1}$ as is shown by red lines connecting the data points with the plane. The parameters of the fits are listed in Table I.

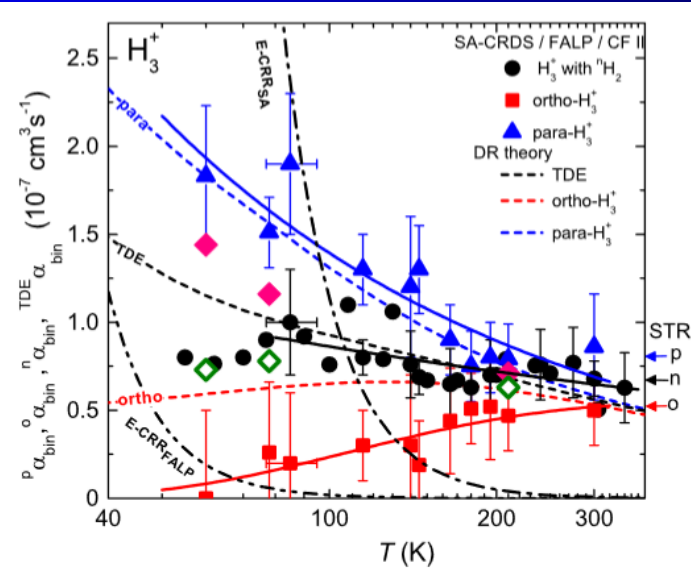


FIG. 8. Cryo-FALP II and SA-CRDS. Nuclear spin state-specific binary recombination rate coefficients measured in Cryo-FALP II, FALP, and SA-CRDS experiments. Triangles and squares indicate ${}^p\alpha_{\text{bin}}$ and ${}^o\alpha_{\text{bin}}$, respectively. The values at 85 K, 140 K, 165 K, and 195 K were taken from our previous experiments.¹⁹ The values of ${}^n\alpha_{\text{bin}}$ (circles) were measured in the Cryo-FALP II, FALP, and SA-CRDS experiments and some data were taken from our previous studies.^{19,41} The diamonds refer to ${}^n\alpha_{\text{bin}}$ (open diamonds) and ${}^e\alpha_{\text{bin}}$ (closed diamonds) measured in the present Cryo-FALP II experiment. The full lines are fits to ${}^p\alpha_{\text{bin}}$, ${}^o\alpha_{\text{bin}}$, and ${}^n\alpha_{\text{bin}}$ to the function in Eq. (7) that is used in astrophysical databases. For details and for the parameters of the fits see the text and Table II. The arrows on the right hand side of the figure denoted as p, o, and n indicate the values of ${}^p\alpha_{\text{bin}}$, ${}^o\alpha_{\text{bin}}$, and ${}^n\alpha_{\text{bin}}$ obtained in CRYRING.¹³ The dashed lines indicated as para, ortho, and thermodynamic equilibrium (TDE) are theoretical dependences for para- H_3^+ , ortho- H_3^+ , and for H_3^+ ions in TDE.^{33,35} The dashed-dotted lines E-CRR_{SA} and E-CRR_{FALP} are effective binary rate coefficients of ternary E-CRR calculated for electron number densities $n_e(\text{SA-CRDS}) = 3 \times 10^{10} \text{ cm}^{-3}$ and $n_e(\text{Cryo-FALP II}) = 5 \times 10^8 \text{ cm}^{-3}$.^{19,27–29}

H_3^+ interaction with e^-

THE JOURNAL OF CHEMICAL PHYSICS 136, 244304 (2012)

Binary and ternary recombination of para- H_3^+ and ortho- H_3^+ with electrons: State selective study at 77–200 K

Petr Dohnal,¹ Michal Hejduk,¹ Jozef Varju,¹ Peter Rubovič,¹ Štěpán Roučka,¹ Tomáš Kotrík,¹ Radek Plašík,¹ Juraj Glosík,¹ and Rainer Johnsen²

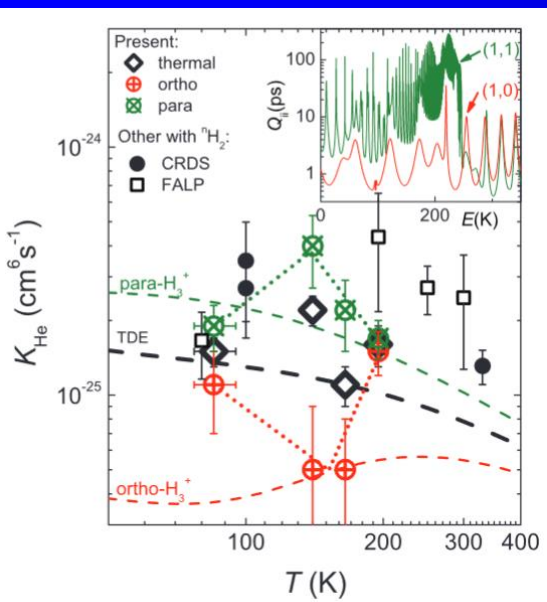


FIG. 12. Ternary recombination rate coefficients ${}^0K_{\text{He}}$, ${}^1K_{\text{He}}$, and ${}^2K_{\text{He}}$. The data obtained in previous CRDS (closed circles) and FALP/SA (open squares) experiments^{33,34} are also shown. The dotted lines drawn through the para and ortho data are only meant to guide the eye. In the insert diagonal elements Q_{ii} of lifetime Matrix Q for the two lowest initial rotational states of H_3^+ are plotted. Each curve is labeled with the corresponding quantum numbers (J.G.).^{8,34}

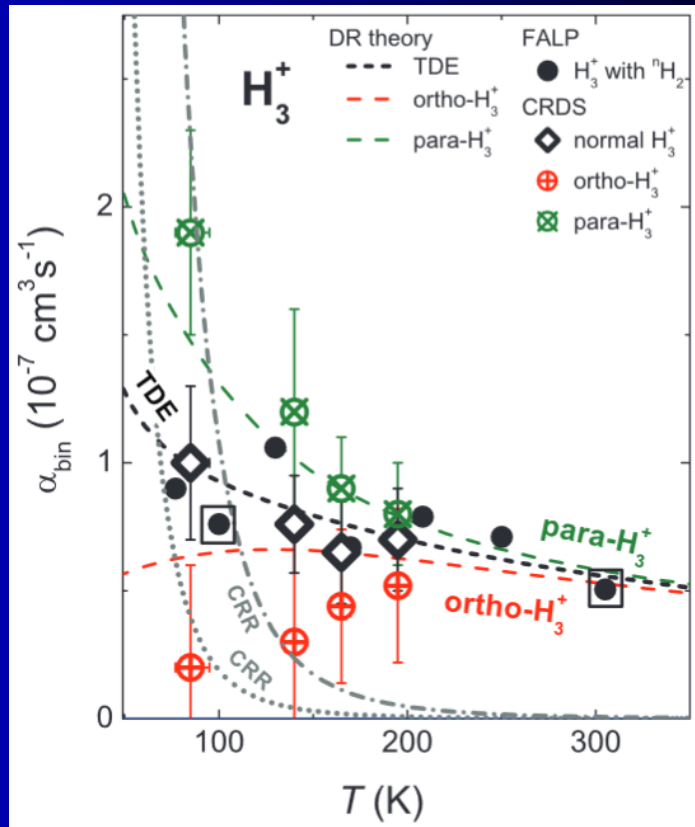
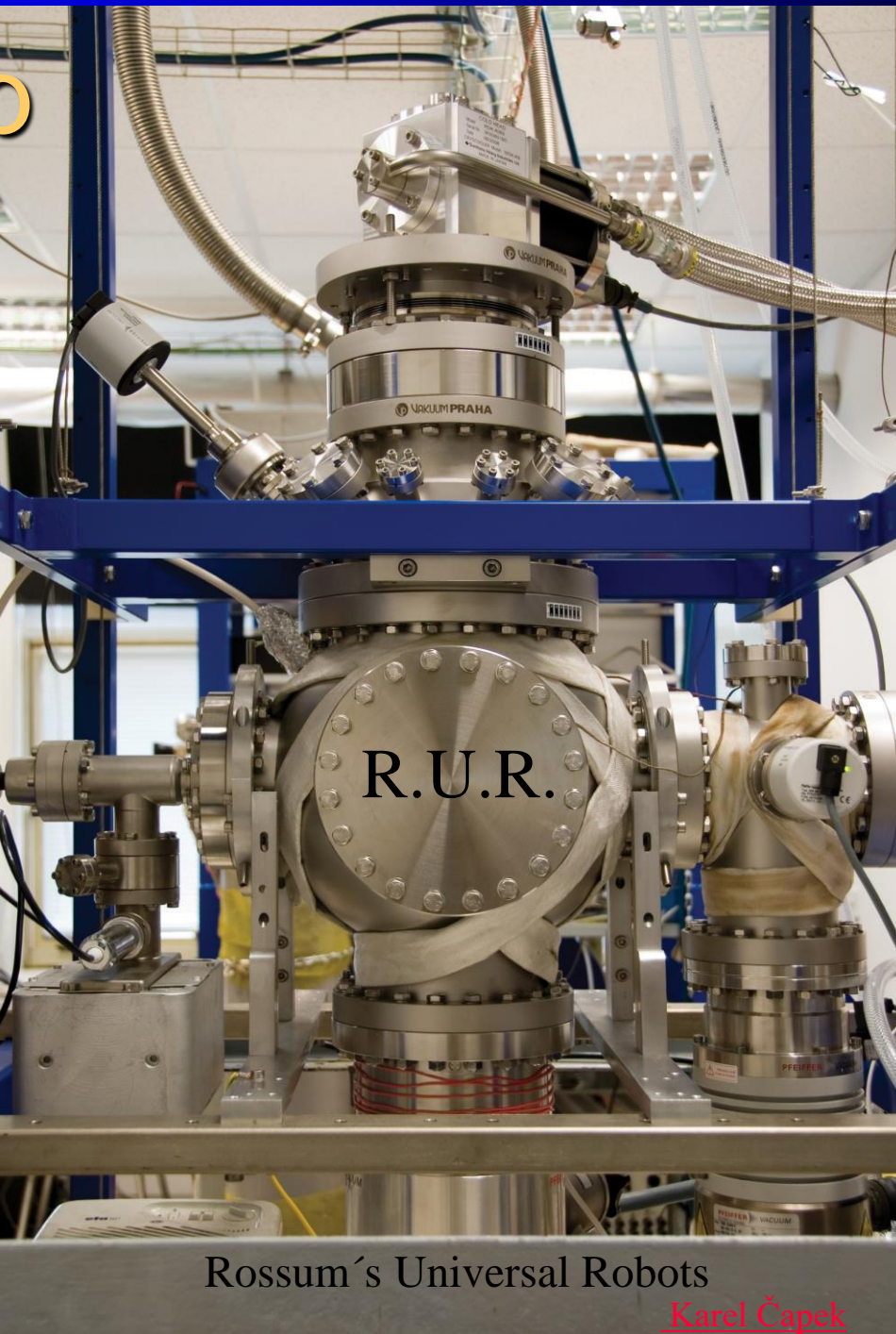


FIG. 13. Measured temperature dependences of the binary recombination rate coefficients ${}^0\alpha_{\text{bin}}$, ${}^1\alpha_{\text{bin}}$, and ${}^2\alpha_{\text{bin}}$ for normal- H_3^+ (measured in experiments with $n\text{H}_2$), para- H_3^+ , and ortho- H_3^+ , respectively (see also Ref. 78). Previous FALP data^{8,33,34} measured with $n\text{H}_2$ are indicated by full circles. Combined SA-CRDS/FALP data at 100 K and 305 K (Refs. 8 and 34) are indicated by a full circle in a square. The temperature T in the SA-CRDS experiments is given by T_{kin} , while in the FALP it is the temperature of the flow tube. That is why we use $T = 82$ K for data obtained in experiment made with discharge tube (SA-CRDS) immersed in liquid nitrogen, otherwise we indicate it as 77 K (e.g., in Fig. 5). Error bars (present CRDS data) represent statistical errors (see linear fits in Figs. 10 and 11). The dashed lines indicate the theoretical rate coefficients for para- H_3^+ , ortho- H_3^+ , and for H_3^+ ions in the thermal equilibrium (TDE).⁶ The curves labeled CRR are the effective binary rate coefficients of collisional radiative recombination (CRR) calculated from the Steffens formula (see Refs. 31, 32, and 38) for electron densities $n_e = 5 \times 10^9 \text{ cm}^{-3}$ (dotted line) and $n_e = 3 \times 10^{10} \text{ cm}^{-3}$ (dash-dotted line). For details see the Appendix.

Electron trap



Rossum´s Universal Robots

Karel Čapek